USGS
science for a changing world

Effects of Including Surface Depressions in the Application of the Precipitation-Runoff Modeling System in the Upper Flint River Basin, Georgia

Scientific Investigations Report 2010–5062

U.S. Department of the Interior
U.S. Geological Survey

Effects of Including Surface Depressions in the Application of the Precipitation-Runoff Modeling System in the Upper Flint River Basin, Georgia

By Roland J. Viger, Lauren E. Hay, John W. Jones, and Gary R. Buell

Scientific Investigations Report 2010–5062

U.S. Department of the Interior
U.S. Geological Survey

U.S. Department of the Interior
KEN SALAZAR, Secretary

U.S. Geological Survey
Marcia K. McNutt, Director

U.S. Geological Survey, Reston, Virginia: 2010

Suggested citation:
Viger, R.J., Hay, L.E., Jones, J.W., and Buell, G.R., 2010, Effects of including surface depressions in the application of the Precipitation-Runoff Modeling System in the Upper Flint River Basin, Georgia: U.S. Geological Survey Scientific Investigations Report 2010–5062, 36 p.

Contents

Figures

Tables

Conversion Factors

SI to Inch/Pound

Multiply	By	To obtain
	Length	
nanometer (nm)	3.937007874016E-8	inch (in)
millimeter (mm)	25.4	inch (in)
meter (m)	3.28083	foot (ft)
	Area	
square kilometer (km^2)	247.1	acre
square kilometer (km^2)	.3861	square mile (mi^2)
	Volume	
cubic meter (m^3)	35.31	cubic foot (ft^3)
cubic meter (m^3)	.0008107	acre-foot (acre-ft)
	Flow rate	
cubic meter per second (m^3/s)	70.07	acre-foot per day (acre-ft/d)
cubic meter per second (m^3/s)	35.31	cubic foot per second (ft^3/s)
	Heat Density	
joule per square meter (J/ m^2)	.000023901	langley (ly)
	Hydraulic conductivity	
meter per second (m/s)	3.281	foot per second (ft/s)
	Permeability	
square meters (m^2)	1.01325E12	darcy (darcy)
darcy (darcy)	0.98692 E-12	square meters (m^2)

Temperature in degrees Celsius (°C) may be converted to degrees Fahrenheit (°F) as follows:

$$°F=(1.8×°C)+32$$

Temperature in degrees Fahrenheit (°F) may be converted to degrees Celsius (°C) as follows:

$$°C=(°F-32)/1.8$$

Vertical coordinate information is referenced to the National Geodetic Vertical Datum of 1929 (NGVD29).

Horizontal coordinate information is referenced to the World Geodetic Survey Datum of 1984 (WGS84).

Altitude, as used in this report, refers to distance above the vertical datum.

Acronyms and Abbreviations

Acronym or abbreviation	Definition
COOP	Cooperative Observer Program
DEM	Digital elevation model
ETM+	Enhance Thematic Mapper Plus imagery
GIS	Geographic information system
HRU	Hydrologic Response Unit
NED	National Elevation Dataset
NHD	National Hydrography Dataset
NID	National Inventory of Dams
NLCD	National Land Cover Database
NRCS	Natural Resources Conservation Service
NS	Nash-Sutcliffe goodness of fit
NOAA	National Oceanic and Atmospheric Administration
NWS	National Weather Service
PET	Potential evapotranspiration
PRMS	Precipitation-Runoff Modeling System
SR	Solar radiation
USGS	U.S. Geological Survey
WATSTORE	Water data storage and retrieval system
WY	Water year

Effects of Including Surface Depressions in the Application of the Precipitation-Runoff Modeling System in the Upper Flint River Basin, Georgia

By Roland J. Viger, Lauren E. Hay, John W. Jones, and Gary R. Buell

Abstract

This report documents an extension of the Precipitation Runoff Modeling System that accounts for the effect of a large number of water-holding depressions in the land surface on the hydrologic response of a basin. Several techniques for developing the inputs needed by this extension also are presented. These techniques include the delineation of the surface depressions, the generation of volume estimates for the surface depressions, and the derivation of model parameters required to describe these surface depressions. This extension is valuable for applications in basins where surface depressions are too small or numerous to conveniently model as discrete spatial units, but where the aggregated storage capacity of these units is large enough to have a substantial effect on streamflow. In addition, this report documents several new model concepts that were evaluated in conjunction with the depression storage functionality, including: "hydrologically effective" imperviousness, rates of hydraulic conductivity, and daily streamflow routing.

All of these techniques are demonstrated as part of an application in the Upper Flint River Basin, Georgia. Simulated solar radiation, potential evapotranspiration, and water balances match observations well, with small errors for the first two simulated data in June and August because of differences in temperatures from the calibration and evaluation periods for those months. Daily runoff simulations show increasing accuracy with streamflow and a good fit overall. Including surface depression storage in the model has the effect of decreasing daily streamflow for all but the lowest flow values. The report discusses the choices and resultant effects involved in delineating and parameterizing these features. The remaining enhancements to the model and its application provide a more realistic description of basin geography and hydrology that serve to constrain the calibration process to more physically realistic parameter values.

Introduction

The U.S. Geological Survey (USGS) Precipitation Runoff Modeling System (PRMS) is a distributed-parameter, physically based hydrologic model. Distributed parameter capabilities are provided by partitioning the study basin into Hydrologic Response Units (HRUs). The original version of PRMS (Leavesley and others, 1983) did not account for the presence of depressions in the land surface that are capable of capturing runoff. In geographic domains where there is a substantial volume of storage capacity created by depressions in the land surface, developing an application of PRMS that accurately reflects hydrologic response can be difficult. To overcome this, an extension of the original model for quantifying and simulating the hydrologic effect of surface-depression water storage is described in this report. This extension builds on the work of several other USGS reports (Steuer and Hunt, 2001; Vining, 2002). The effectiveness is demonstrated by an application in the Upper Flint River Basin in central Georgia (fig. 1). This extension is valuable for applications in basins where runoff-capturing depressions in the land surface are too small, numerous, or both, to conveniently model as discrete spatial units but where the aggregated storage capacity of these units is large enough to have a substantial effect on watershed hydrology. A surface depression does not need to be a perennial water body; it is simply a topographic feature that is capable of slowing, storing, or redirecting surface runoff and therefore modifying the streamflow response.

The Flint River Basin was chosen as a complement to the ongoing work of "the Flint River Science Thrust Project of the U.S. Geological Survey, part of a federally funded program to address key national science priorities including landslides and debris flows, fire science, integrated landscape monitoring, and water availability. The purpose of the Flint River Science Thrust Project is to advance the science needed to specify the hydrologic conditions necessary to support flowing-water ecosystems. This information is critical for management of water supplies" (Hughes and others, 2007, p. 1).

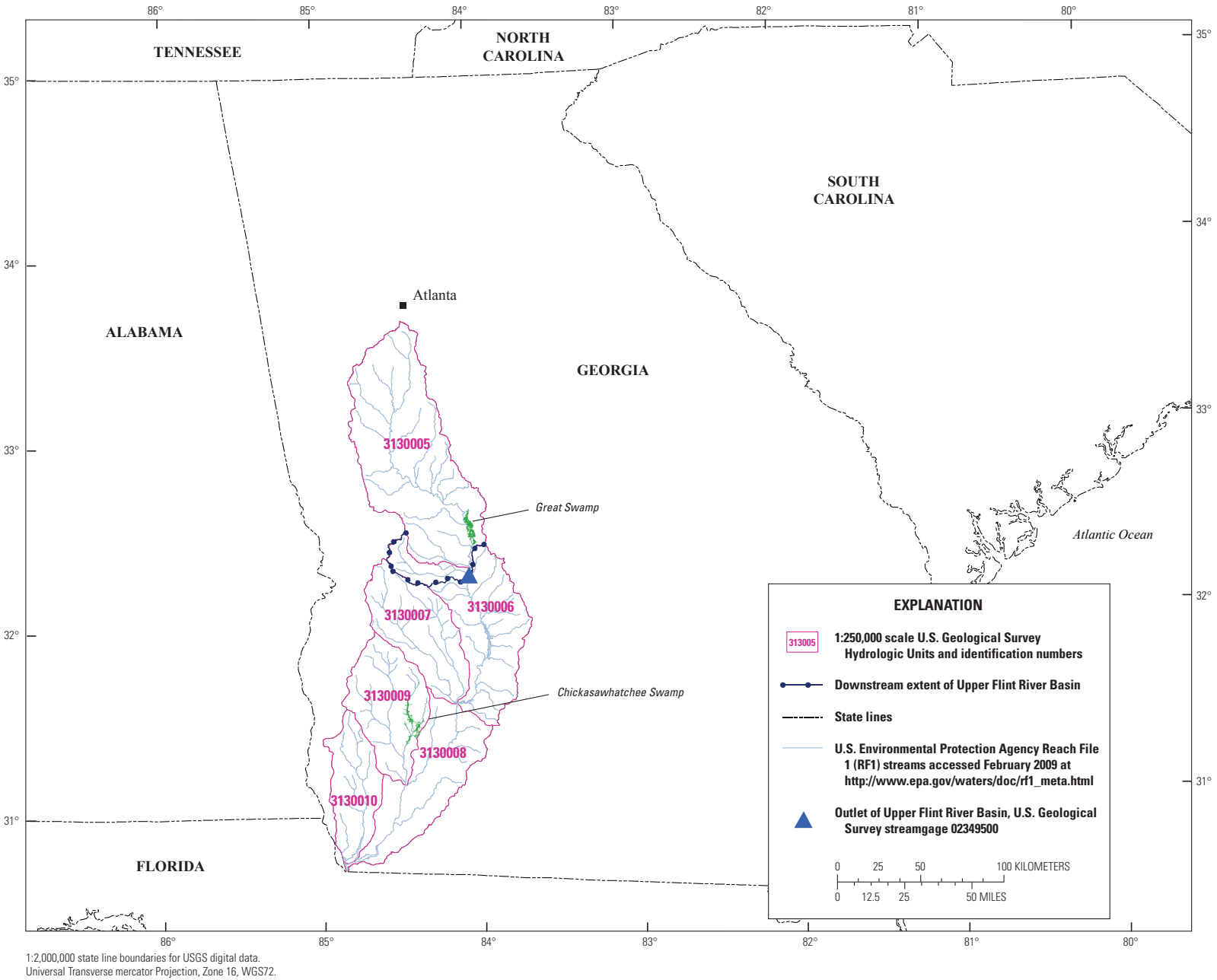

Figure 1. Hydrologic Units associated with the Flint River Basin, Georgia. The Upper Flint River Basin includes Hydrologic Unit 03130005 and part of 03130006, above the U.S. Geological Survey streamgage, 02349500.

Examination of remotely sensed imagery of the landscape in the Upper Flint River Basin revealed the presence of numerous small surface depressions capable of capturing and holding runoff. Many of these are ponds that had been constructed along rivers to help power grist mills. This interpretation is consistent with a variety of sources stating that mill ponds had been built "by the thousands" (Dean, 2008). Literature describing the history of the State of Georgia indicates that there were almost 1,200 water-powered mills, each presumably with an associated dam, within the State (Northeast Georgia Mountain Travel Association, 2005). These mills were so prevalent on the southeastern landscape that they were inventoried by the U.S. Geological Survey in a report on water power in the State of Alabama (Hall, 1904). The ponds associated with the mills were sometimes large, serving as community resources for fishing and hunting (Owen, 1921). Some researchers contend that these mill ponds were so numerous that most flood plains on the eastern coast of the United States are actually fill terraces formed by sediment dropped by still waters in these ponds (Walter and Merritts, 2008).

In addition, the U.S. Department of Agriculture, Natural Resource Conservation Service (NRCS) has had a long history of encouraging the development, preservation, and restoration of wetlands, farm ponds, and other water bodies on private lands for a large range of farming and environmental purposes. These include control of water supply, flood control, management of sedimentation, and the quality of water that is delivered to streams, erosion of topsoil, protection of wildlife, and sustaining recreation (Natural Resources Conservation Services, 1996). Many state and local soil and water conservation districts also have long encouraged creating and using small ponds as part of a land management strategy.

Even after the earthen dams used to form these ponds give way, they leave definite artifacts on the landscape, in the form of surface depressions, capable of capturing and storing volumes of water. Although no exact accounting of farm or mill ponds exists for the Flint River basin or within the State of Georgia, several national and global inventories of small, artificial water bodies have been carried out. One method, on the basis of the National Land Cover Dataset (NLCD) (Vogelmann and others, 2001), resulted in an estimate of 2.6 million ponds in the United States (Smith and others, 2002). Smith and others (2002) show that smaller water bodies constitute a large proportion of the total number of water bodies across the United States (fig. 2*A*). These small water bodies collectively represent a large percentage of the total surface area of all water bodies in the country (fig. 2*B*).

Another study, which used 1:24,000 scale topographic quadrangles, resulted in an estimate of 8–9 million ponds in the U.S. (Renwick and others, 2005). Renwick and others (2005) report that 21 percent of the total surface area in the United States drains into such small, artificial ponds. Although these authors did not derive the volume of storage associated with these water bodies, it is still clear that these features must collectively have an important effect on the streamflow response of a basin.

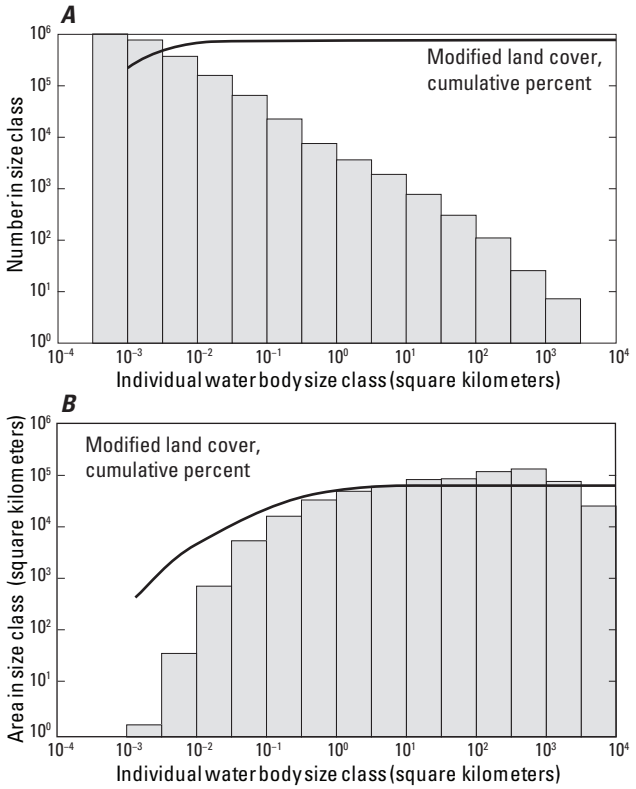

Figure 2. Possible aggregated number and area for different size classes of water bodies within the United States (modified from Smith and others, 2002).

Dedicating an HRU to each surface depression unit generally is not practical; the area of each of these units would be so small that the derivation of information specific to each one would rely on inappropriately small numbers of cells from the best available geographic information system (GIS) data (1–5 cells from a raster elevation data set with a cell size of 10 meters, for example). From the perspective of GIS analysis, few if any standard spatial data sets have the resolution from which to extract or describe these features. This constraint forces the use of an HRU resolution that inevitably results in a degree of heterogeneity in the character of each HRU. While the extension described here does not eliminate this heterogeneity, it attempts to make explicit the occurrence of small surface depressions within an HRU.

Purpose and Scope

The purpose of this report is to document an extension made to PRMS for simulating the hydrological effects of surface depressions on basin streamflow, for simulating streamflow routing at a daily time step, and methods for deriving parameters used to drive these simulations. In addition, this report presents methods for estimating parameters describing "hydrologically effective" imperviousness and rates of hydraulic conductivity. This report also demonstrates the effectiveness of these enhancements and methods in an application to the Upper Flint River Basin.

Study Area

The Flint River system is one of only 40 rivers within the conterminous United States that flows unimpeded for more than 320 kilometers (Morris, 2005). It contains many water holding surface depressions, including officially designated wetland areas such as the Great Swamp and the Chickasawhatchee Swamp, and supports a diversity of plant and animal life. The Flint River has its headwaters in northern Georgia, emanating from a groundwater source—now through a concrete culvert that routes flow underneath the Hartsfield-Jackson Atlanta International Airport (Morris, 2005). The main physiographic province of this source is the Southern Piedmont region. The river, downstream from Montezuma, Georgia, passes through the Coastal Plains physiographic region as it joins the Chattahoochee River and ultimately drains into the Gulf of Mexico. The Flint River also is important to human populations because it is a major water supply for the states of Alabama, Georgia, and Florida and because it has flooded several cities that lie along its path. While early industry in the region was dominated by grist mills, irrigation-based agriculture now is important (Morris, 2005). Crops include peanuts, soybeans, and vegetables. Dairy, cattle, and hogs also are important agricultural commodities for the area. General patterns of water use in the basin were not considered hydrologically significant for this study.

The surface depression water-storage routine that has been added to PRMS is demonstrated by an application to the Upper Flint River Basin above USGS streamgage 02349500 at Montezuma, in Macon County, Georgia. The contributing area above this gage terminates in the upper end of Hydrologic Unit 03130006 and includes the upstream Hydrologic Unit 03130005, as shown in figure 1. This basin has a drainage area of approximately 7,511 square kilometers. The mean basin elevation is 233 meters above the National Geodetic Vertical Datum of 1929. The basin is predominantly forested (≈73 percent), although there is notable recent urbanization in the northern headwaters. The most substantial urbanization in the basin is the result of expansion of southern suburbs surrounding the Atlanta metro area, although several smaller cities also are growing along downstream portions of the river.

Previous estimates of surface-depression water storage within the basin are 0.65 percent of total basin area (Slack and Landwehr, 1992; Slack and others, 1993). This estimate, taken from the USGS WATSTORE basin characteristics data (Dempster, 1983), was on the basis of analyses described in (Thomas and Benson, 1970). The current study determined that 2.45 percent of the basin area was covered by surface depressions, on the basis of image processing and GIS analysis of high resolution imagery. The derivation of the surface-depression map is discussed in detail in the "Mapping Surface Depression from Remotely Sensed Data" section of this report.

Daily maximum and minimum temperature and precipitation data from stations in and around the Upper Flint River Basin were compiled from 28 measurement stations from the National Oceanic and Atmospheric Administration (NOAA) Cooperative network (COOP; National Oceanic and Atmospheric Administration Cooperative Observer Program, 2009). Figure 3 shows mean monthly values of basin maximum and minimum temperature, precipitation, and streamflow for the water years 1988–1999. The highest mean monthly temperatures are seen in the month of July and the lowest are in December and January. Mean monthly precipitation is highly variable. Highest mean monthly values of streamflow are seen in March with another peak in July because of the large precipitation events seen in that month for this period of record. The lowest mean monthly values of streamflow occur in September (U.S. Geological Survey National Water Information System, 2009).

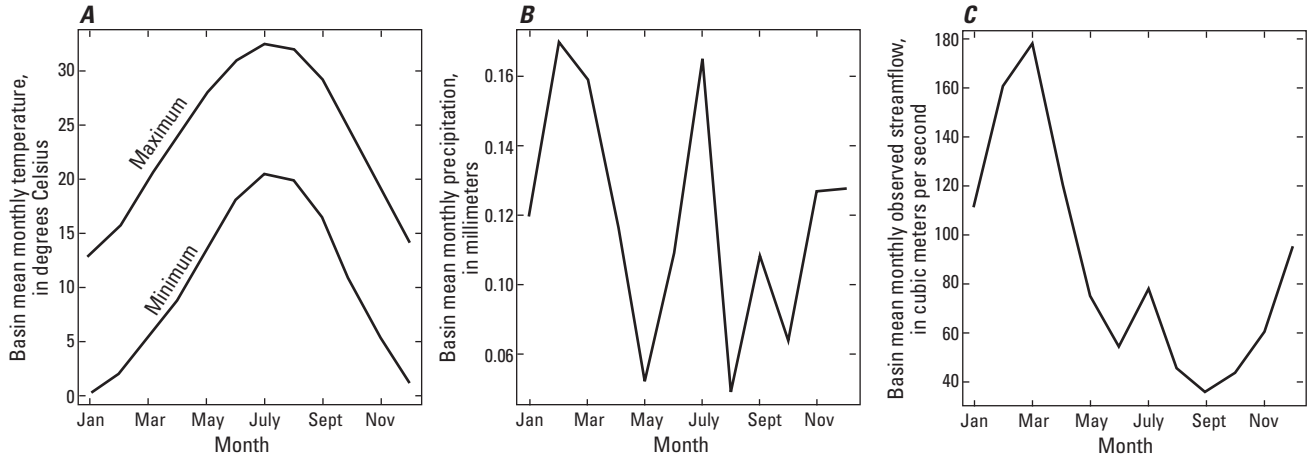

Figure 3. Basin mean monthly (*A*) maximum and minimum temperature, (*B*) precipitation, and (*C*) measured streamflow at U.S. Geological Survey streamgage 02349500 for water years 1988–1999.

Previous Studies

Steuer and Hunt (2001) used PRMS in a study that evaluated the hypothetical installation of several detention ponds to offset increased runoff produced by urbanization. These authors manually assessed topography and soils information to locate prospective detention-pond sites and generate volume estimates for the ponds. These volumes were compared to PRMS-simulated inflows to the pond areas and illustrated an important deficiency in PRMS—the lack of daily accounting for storage in surface depressions within an HRU or the enclosing basin. In contrast to the study presented here, Steuer and Hunt (2001) handled a small number of relatively large water bodies.

Vining (2002) examined the hydrologic behavior of a basin that contained substantial areas of surface depressions in North Dakota (prairie potholes, in particular). The project developed a modified version of PRMS (the "Devils Lake Basin wetlands model"). It aggregated surface depressions on a per HRU basis and used a stream network to route overland flow within the basin.

The surface depressions described by Vining (2002) were determined by using a manually created high resolution (10-meter cell size) raster elevation data set (DEM) and the GIS Weasel software package (Viger and Leavesley, 2007). It was assumed that elevations in the DEM accurately reflected the height of the land surface below any standing water. On the basis of this assumption, a new DEM was derived by raising the height of each depression until gravity driven flow across the land surface could be resolved by using standard GIS analyses. Estimates of maximum wetland area were determined by differencing the original and the "filled" DEM.

This studies highlights the difficulty of relying on elevation data to determine surface depression areas. The size of the features may be substantially smaller than the sample spacing used for the elevation data. Depending on where the elevation measurement is taken, features smaller than a cell may not be detected by using the DEM. Also, errors in the elevation data that stem from a number of sources (for example, the original production process, boundary or tile discontinuities, and the interpolation used to resample or reproject the elevation data) can introduce spurious depressions. Another problem with relying on elevation data alone to generate this input is the uncertainty as to whether the elevation postings in the data set depict the land surface beneath a water body or the water surface.

Model Conceptualization and Parameterization

PRMS conceptualizes (fig. 4) the hydrology at and below ground-level as a series of reservoirs (impervious zone, soil zone, subsurface, and groundwater) whose outputs combine to produce streamflow. Each HRU includes, in addition to a near-surface soil zone, a plant canopy and a snowpack component or reservoir. For each HRU, a water balance is computed each day and an energy balance is computed twice each day.

The DEM used to develop the HRUs and parameterize the model was downloaded from the U.S. Geological Survey National Map Seamless server (http://seamless.usgs.gov, accessed March 2007). The scale of the downloaded DEM data was 1 Arc Second from the National Elevation Dataset (NED), which was projected into the Albers coordinate system (Meades Ranch, Kans., configuration) for this study. Because this DEM was higher resolution (≈30 meter cell size) than was deemed necessary for this study, the DEM was resampled to a 100-meter cell size.

A representation of the Upper Flint River stream network was created by extracting all DEM cells with a contributing area exceeding 35 square kilometers. Each link in the network (between a headwater and a confluence, between two confluences, or between a confluence and the basin outlet) was uniquely identified with identification numbers increasing in a downstream order. A number of subjective changes were made to this initial stream network:

1. To ensure that certain known water bodies would have a nearby stream segment,
2. To break pre-existing segments on the basis of known points of interest (such as streamgages or reservoir outlets) for model calibration or water management, and
3. To group smaller segments together to simplify parameter generation.

Figure 5 shows the drainage density of the final derived stream network. For the purpose of this study, the representation of the stream network does not need to precisely recreate the path of perennial or ephemeral streams as found in the field. It is a representation designed to create a drainage network whose structure was sufficiently accurate for accumulating, directing, and controlling the timing of stream-based flow on its way to the basin outlet. HRUs were delineated as the contributing areas to each segment in the stream segment map.

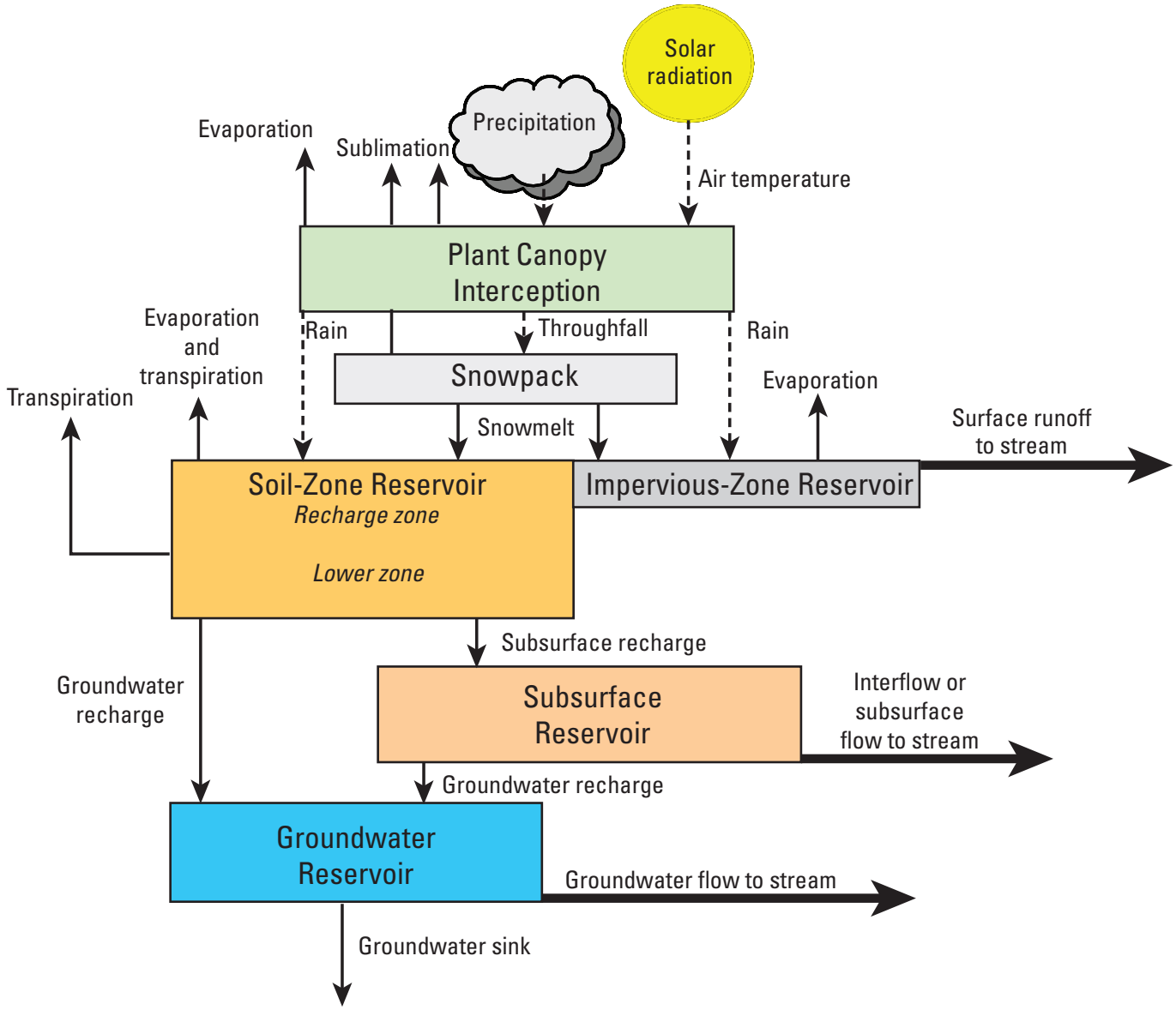

Figure 4. Overview of the Precipitation-Runoff Modeling System conceptualization of basin components and fluxes (taken from Markstrom and others, 2008).

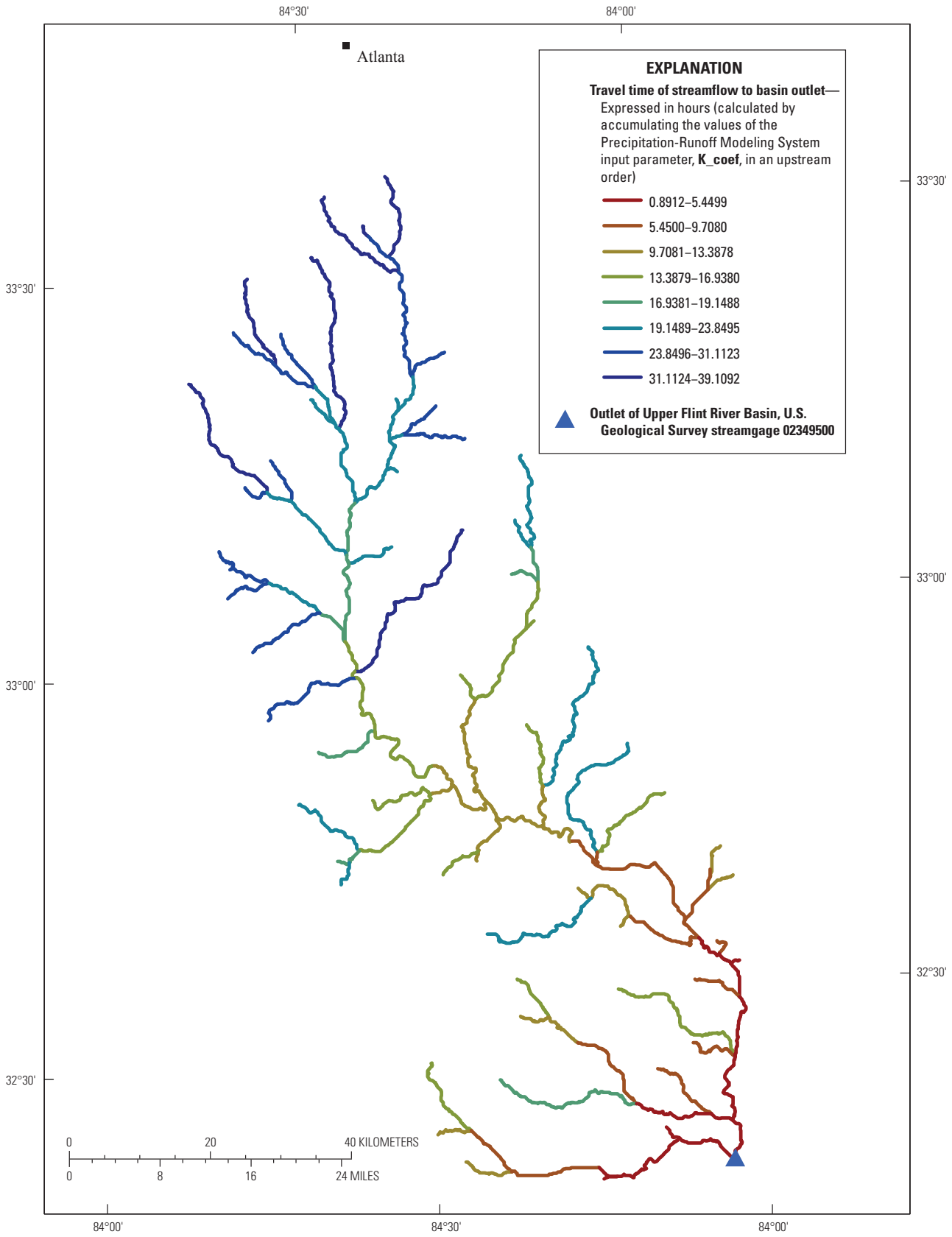

Figure 5. Stream network derived for the study. The color of a segment represents the number of hours it takes water in that segment to reach the outlet. This was calculated by accumulating the values of the Precipitation-Runoff Modeling System input parameter, **K_coef**, in an upstream order.

In many PRMS applications, HRUs are defined by breaking the contributing areas into "left-bank" and "right-bank" areas for the benefit of more accurate simulation of energy and therefore snowmelt processes. As snow does not accumulate in this basin, the single contributing area method of HRU delineation was deemed sufficient. Figure 6 shows the map of HRUs used in this study.

The following sections provide an introduction to the portions of the model that are being highlighted in this report. Model conceptualization and parameterization are described for simulating:

1. Surface depressions,
2. Impervious and partially impervious surfaces,
3. Hydrologic fluxes out of the HRU soil zone, and
4. Streamflow routing.

Surface Depressions

The following three subsections describe the concepts to support the simulation of surface-depression water storage processes. The first section, "General Hydrology Related to Surface-Depression Storage," highlights the concepts to simulate the hydrology associated with surface depressions. The section, "Mapping Surface Depressions from Remotely Sensed Data," explains the procedures used to detect surface depressions by using remotely sensed imagery. The third section, "Surface-Depression Parameters," provides the definition and procedures used to estimate each piece of information used to describe an HRU's surface depressions in PRMS.

General Hydrology Related to Surface-Depression Storage

The contribution to streamflow from each HRU is calculated by PRMS at a daily time step as the sum of the surface runoff, subsurface, and groundwater outflows. Water stored in surface depressions can modify each of these components. The aggregated volume of water held by all the surface depressions within an HRU is a function of the HRU surface-depression storage capacity and the hydrologic conditions (inflow, precipitation, evaporation, seepage to groundwater, and outflow) at that time. The surface area of the open water on an HRU is a function of the computed storage volume at each time step.

Precipitation or snowmelt occurring on surface depressions adds to the stored volume of water in those surface depressions. Precipitation and snowmelt occurring on nondepression areas of an HRU are assumed to infiltrate, run off, or both, into the stream channel adjacent to the HRU or into surface depressions within the same HRU, depending on how the HRU has been parameterized. Surface runoff is computed as a function of antecedent soil-moisture conditions, total soil-moisture capacity, and precipitation volume incidental to the HRU within the time step. Infiltration is computed as the difference between net precipitation (total precipitation minus precipitation stored on vegetation cover) and surface runoff. Evapotranspiration from the soil areas of an HRU is computed as a function of potential evapotranspiration, soil texture, and the amount of water available in the soil profile.

Mapping Surface Depressions from Remotely Sensed Data

This study used remotely sensed imagery to estimate surface-depression locations and area. While it would be possible to visually delineate surface depressions on high-resolution orthophotography, the amount of effort involved makes the process cost prohibitive. Digital processing of orthophotography also is expensive, given requirements for color balancing (to allow sufficient accuracy), compositing, storage, and manipulation of the imagery. Therefore, techniques that make use of digital processing of satellite imagery were explored for mapping surface depressions within the Upper Flint River Basin, while individual digital orthophotographs were used to assess the quality of the satellite-based maps. Imagery-based mapping and monitoring of water bodies has been conducted elsewhere (for example, Armenakis, 2007; Chipman and Lillesand, 2007; Vanderbilt and others, 2007). However, in all previous applications, the targeted water bodies are much larger than the surface depressions being analyzed here.

For this study, a spring (April 14, 2003) Landsat 7 Enhanced Thematic Mapper (ETM+) image was selected to ensure relatively wet antecedent weather conditions, clarity of the image (that is, there was little atmospheric contamination of the image on that date), and its capture prior to the failure of the scan line corrector (U.S. Geological Survey, 2009). Wet conditions were sought to increase the likelihood that the water storage in surface depressions would have the largest possible areal extent. An ETM+ image consists of 6 bands covering the reflected light spectrum (blue through middle-infrared) at nominal 30-meter ground resolution, 2 thermal-emission bands at nominal 60-meter ground resolution, and a panchromatic reflected-light (blue through near-infrared) band at nominal 15-meter ground resolution (National Aeronautics and Space Administration, 2009).

Initial efforts focused on the delineation of the surface area of water stored in surface depressions by using techniques designed to estimate the proportion of various land-cover types within individual cells of Landsat measurement (that is, "pixels" that are nominally 30 meters on each side) from the multispectral data. However, this process was sensitive to soil moisture and shadow and incorrectly identified wet bare soil and shadowed areas as water surfaces. Mixed forest canopy covers much of the Upper Flint River Basin and frequent shadowing within canopy gaps, spectrally similar to small water bodies, resulted in large overestimation of water bodies. With continued experimentation, a much simpler approach was developed.

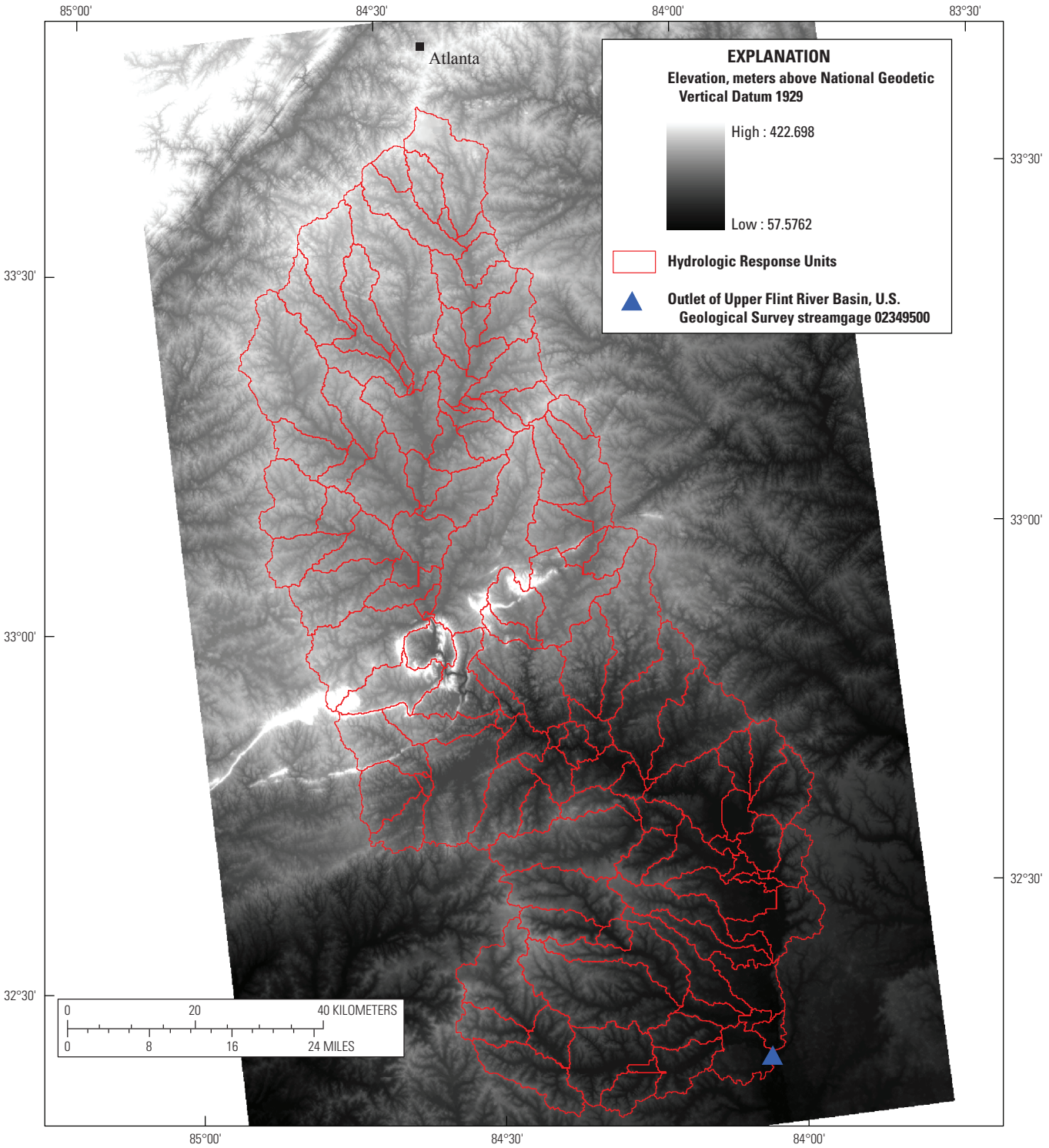

Figure 6. Hydrologic Response Unit map derived for the study, superimposed on a digital elevation model for the area.

For map development, the ETM+ panchromatic band was iteratively classified as "water" or "nonwater" through a technique referred to as image thresholding. This is a simple, interactive technique that can be employed by using widely available GIS software operations. The operator instructs the software to code all cells with values below a selected threshold to "1" (or "water") and all those with values above the threshold to "0" ("nonwater") in an iterative fashion until a suitable data set is produced. This approach is based on the reflectance characteristics of water as represented by ETM+ panchromatic data. The ETM+ panchromatic band records reflectance in the range of 520 to 900 nanometers (nm). Because water strongly absorbs light, particularly in the near-infrared region (700–900 nm), it is useful for land and water discrimination, and 15-m pixels with the lowest reflectance values typically are water. Through comparison against high-resolution orthophotographs, it was possible to select an ETM+ panchromatic band value that detected water storage in surface depressions without also selecting a substantial number of shadowed forest or wet bare-soil areas that were a source of confusion for more complex mapping procedures. With limited experimentation, a threshold satellite digital number value (applicable only to the image in question without further calibration) was set to 45. Results of the surface depression mapping process are shown in figure 7*A*, with an enlargement of an area at the northern portion of the basin in figure 7*B*.

Surface-Depression Parameters

The surface-depression storage-parameter names, dimensions, description, default values and ranges are shown in tables 1 and 2. Table 1 lists the parameters that were determined by using GIS and remote-sensing technology. Table 2 lists the parameters that were set initially to default values and calibrated or determined with some prior knowledge. In table 1, the parameters **hru_percent_dprst**, **dprst_pct_open**, **dprst_dem**, and **sro_to_dprst** are used to describe each HRU. These parameters are described below.

hru_percent_dprst The area of an HRU occupied by surface depressions, expressed as a decimal percent of total HRU area. Area of all surface depressions for an HRU is summarized in a single value.

dprst_pct_open The decimal percent of the total area of surface depressions within an HRU that spills into the drainage network. Surface depressions may or may not spill directly into the drainage network. Those that do spill directly into the drainage network are referred to as "open" and those that do not spill directly into the drainage network are "closed," as described in Vining (2002).

dprst_dem The volume of surface depression storage capacity in the HRU, expressed in acre-feet.

At every time step, the volume and area of stored water in the surface depressions are calculated on the basis of what the maximum volume can hold. Water in excess of this parameter is spilled to the stream segment associated with the HRU. This study used the U.S. National Inventory of Dams (NID) (U.S. Army Corps of Engineers, 2007) to develop a regression equation that predicted the volume of a water body on the basis of its surface area. The equation was developed from the NID characteristics, referred to as "surface_area" and "NID_storage" in the database, which described a subset of 265 water bodies located within the same physiographic region as the Flint River basin. Several larger reservoirs (Horton Creek, J.W. Smith Reservoir, Lake Peachtree, Peed Brothers Lake, Whitewater Pond, and two with no name; identified as GA04477, GA03893, GA0236, GA05524, GA0304, GA04476, GA04770, respectively, in the NID database) were manually selected and dropped from the analysis because the area-volume relations of these features were not representative of the types of water bodies that the authors sought to describe. The regression that resulted from the remaining data was:

$$sv = 11.01415 * sa, \quad (1)$$

where *sv* is the storage volume, in acre-feet, and *sa* is the reservoir surface area, in acres. The regression fitting forced the derived volume equal to zero when the reservoir area was zero, yielding an r^2 of 0.8593 and a standard error of 0.27578. The storage volume of each delineated surface depression was calculated by using equation 1, and the parameter **dprst_dem** was calculated for each HRU by summing the storage volumes for all surface depressions within each HRU.

sro_to_dprst The percent of the HRU pervious land surface (1 – **hru_percent_imperv**) that flows into depression storage. These two parameters (**sro_to_dprst** and **hru_percent_imperv**), in conjunction with percent of HRU surface area flowing in surface-depression features (**hru_percent_dprst**), help to better define the "effective imperviousness" of the HRU. Rather than assuming that all impervious surface area is immediately hydrologically connected to the drainage network (that is, that any rainfall onto that surface will result in a flash of water arriving nearly instantaneously in the drainage network), the surface-depression storage module first determines what proportion of the impervious surface is upslope from a surface depression.

Using a GIS to derive the areas upslope from each of the originally delineated surface depressions would result in 100 percent of all runoff being captured (expressed in the **sro_to_dprst** parameter). Figure 8*A* shows the HRUs used to simulate hydrology for the basin in black lines. The colored areas within each HRU represent the land surface whose runoff is captured by surface depressions within the HRU. This figure demonstrates that using the derived map of contributing areas to surface depressions with no modification to calculate the **sro_to_dprst** parameter results in almost 100 percent of runoff in all HRUs being captured. In the judgment of the authors, this was not hydrologically realistic. Surface depressions located on or near streams were considered to be part of the drainage network. Therefore, experimentation was done by

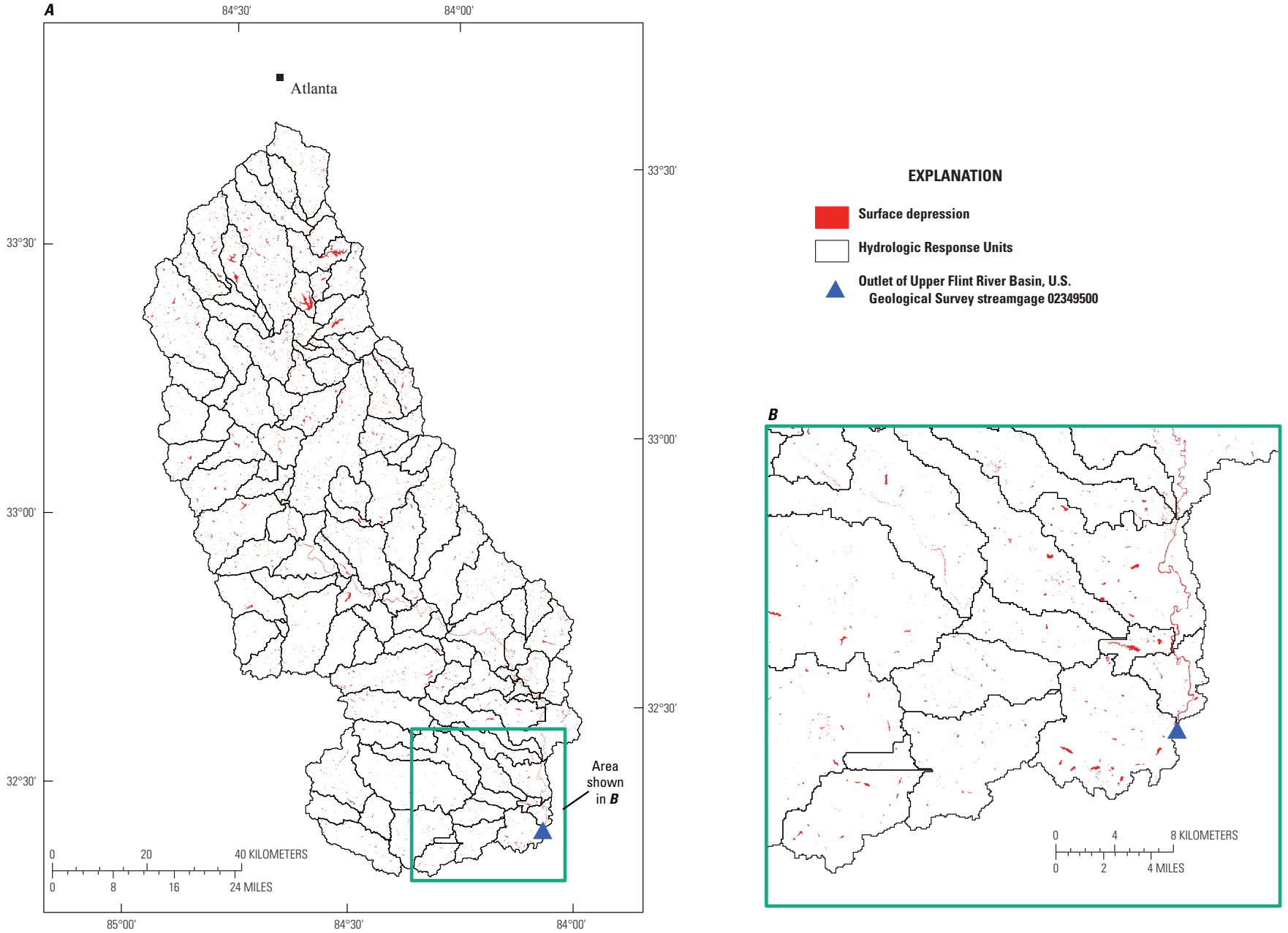

Figure 7. Surface depressions delineated with the analysis of the Enhanced Thematic Mapper Plus data, for: (*A*) the entire Upper Flint River Basin; and (*B*) area near the outlet of the basin, which is outlined with a green box on (*A*).

Table 1. Depression storage parameters derived from geographic information systems analyses.

Parameter	Dimension	Description	Units	Default value (Range)
hru_percent_dprst	nhru	Percent of the Hydrologic Response Unit occupied by depression storage.	Decimal percent	0 (0–1)
dprst_pct_open	nhru	Percent of depression storage area that is hydrologically "open." An open storage feature is one that spills into a stream.	Decimal percent	0 (0–1)
dprst_dem	nhru	Volume of surface depression storage within each Hydrologic Response Unit.	Acre-feet	0 (0–1,000)
sro_to_dprst	nhru	Percent of Hydrologic Response Unit pervious area that flows into Hydrologic Response Unit depression storage.	Decimal percent	0.2 (0–1)

Table 2. Depression storage parameters not derived from geographic information systems analyses.

Parameter	Dimension	Description	Units	Default value (Range)
op_flow_thres	nhru	Percent of maximum open depression storage above which flow occurs.	Decimal percent	0.2 (01)
dprst_pcnt_init	nhru	Initial surface depression storage as a percent of maximum capacity for each Hydrologic Response Unit.	Decimal percent	0.5 (0–1)
dprst_seep_rate	nhru	Coefficient in linear depression storage seepage flow algorithm: **dprst_seep** = **dprst_seep_rate** * **dprst_stor** where **dprst_stor** is current depression storage.	none	0.01 (.0001–1)
va_clos_exp	nhru	Exponent in the volume to surface area relation for closed-depression storage.	none	1.0 (.0001–10)
va_open_exp	nhru	Exponent in the volume to surface area relation for open-depression storage.	none	1.0 (.0001–10)
dprst_flow_coef	nhru	Coefficient in linear depression storage flow routing algorithm.	none	0.01 (.0001–3.0)
dprst_et_coef	nmonth	Coefficient to adjust potential evapotranspiration to lake evaporation.	none	1.0 (.5–1.5)

eliminating some surface depressions on the basis of proximity to the drainage network prior to determining the contributing areas. Therefore, trials to reduce the value of this parameter were evaluated by applying spatial filtering to the map of surface depressions.

Various constraints on the original map of surface depressions were developed; visualizations of alternate estimates of HRU area that drained into surface depressions are shown in figure 8*B–D*. Figure 8*B* shows the contributing areas to all surface depressions, but excludes parts of surface depressions that lie directly on the drainage network (as determined from the DEM). This resulted in a major reduction in the **sro_to_dprst** parameter values. Because of the way HRUs were delineated in this study, most of the flow out of an HRU usually passes through a single point at the downslope end of the stream draining that HRU. If that point is designated as a surface depression, then the **sro_to_dprst** parameter value would indicate that all of the flow out of the HRU would be captured by a surface depression. Excluding this point, as well as other points on the drainage network within the HRU, substantially reduces the **sro_to_dprst** parameter value.

The next trial used only surface depressions at least 300 meters from the drainage network. If an individual surface depression straddled this distance threshold, the portion of the surface depression beyond the limit was still used. The result is shown in figure 8*C*. Figure 8*D* shows the contributing areas to those surface depressions that are entirely beyond the 300 meter distance threshold. If an individual surface depression straddled the limit, it was excluded. The results from figure 8*D* were considered the most hydrologically realistic and used to parameterize the model.

With expert knowledge of the basin hydrology being modeled, the user may be able to refine the range of the parameter values given in table 2. For this study, these parameters were set to their default values (see table 2) and calibrated.

op_flow_thres The threshold, expressed as a proportion of maximum surface-depression storage, above which spillage can occur in each HRU. When the threshold is reached, water is allowed to spill out of the surface depressions.

dprst_pcnt_init The initial surface depression storage, expressed as a proportion of the HRU surface depression storage capacity (**dprst_dem**) for each HRU. PRMS can be used to determine what this initial value should be by examining how long it takes the model to reach some level of equilibrium in the storage volume. This involves running the model by using various values, by selecting the optimal value, and by restarting the simulation with the optimal value.

dprst_seep_rate A linear coefficient in the algorithm simulating seepage from the depression storage for an HRU into the subsurface reservoir.

va_clos_exp and **va_open_exp** Coefficients used in the surface depression area-to-surface depression volume relation for 'closed' (**va_clos_exp**) or 'open' (**va_open_exp**) depression storage. The storage volume in the surface depressions at any given time step of the model simulation is determined by Vining (2002):

$$A_{max} = e^{\,c(\ln V max)}, \qquad (2)$$

where A_{max} is the decimal fraction of the maximum possible surface depression area for each HRU, e is the exponential function, c is the coefficient (which is used to set **va_clos_exp** or **va_open_exp**), and V_{max} is the decimal fraction of the maximum depression storage volume. A minimum value of 0.0001 will result in the calculated surface area being set to the maximum possible surface area.

dprst_flow_coef The rate of spilling from surface depressions in an HRU into the stream. This coefficient is a linear function of actual storage within the HRU surface depressions.

dprst_et_coef This adjusts the potential evapotranspiration occurring over the water stored in the surface depressions. This parameter varies by month.

Impervious and Partially Impervious Surface Concepts and Parameter Preparation

Although this report does not introduce new PRMS parameters related to this topic, it does discuss new ways to develop values for the parameter, **hru_percent_imperv**. This parameter describes the proportion of each HRU that is impervious. Impervious portions of an HRU are assumed to be bare of vegetation; no interception of precipitation will occur in these areas. These impervious surfaces are assumed to have a maximum storage capacity (described for each HRU by the **imperv_stor_max** parameter), which is usually small, that can be depleted by evaporation. Once this capacity is exceeded, runoff is generated and assumed to be routed directly to streams. Figure 4 presents an overview of how PRMS conceptualizes the hydrologic components of a basin and the fluxes between those components.

The volume of precipitation or snowmelt on an impervious area that becomes runoff is assumed to route directly to the stream. When using PRMS, a typical approach to calculating the **hru_percent_imperv** parameter values is to determine the area of impervious surfaces within each HRU as a percent of the total HRU area. This approach reflects that PRMS is most commonly applied to nonurbanized areas and most impervious surfaces are rock outcrops or perennial ice bodies. Because this application includes substantial acreage of urbanized land surfaces, much of it impervious, this approach was modified by including methods to assess whether the movement of runoff from individual patches of impervious land surface to the drainage network would be interrupted by surface depressions. Justification for this approach can be found in a number of other contributions (for example, Alley and Veenhuis, 1983; Zarriello and Barlow, 2002; Wissmar and others, 2004).

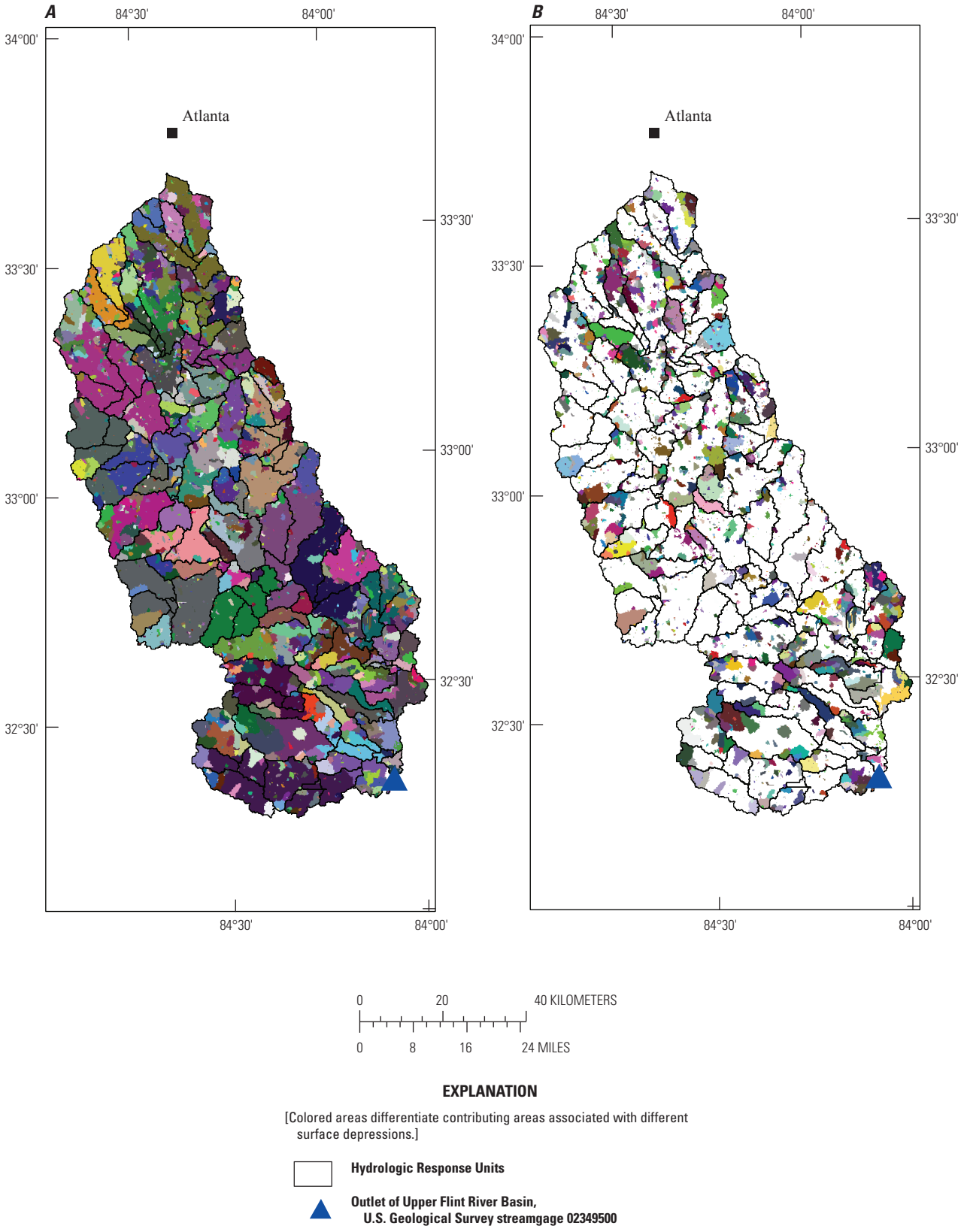

Figure 8. Contributing areas to surface depressions were defined: (*A*) using entirety of surface depressions; (*B*) using nonstream parts of surface depressions; (*C*) using only parts of surface depressions that are at least 300 meters from the streams; and (*D*) using only surface depressions that are entirely 300 meters from streams (that is, if any part of a surface depression is within 300 meters, it is excluded).

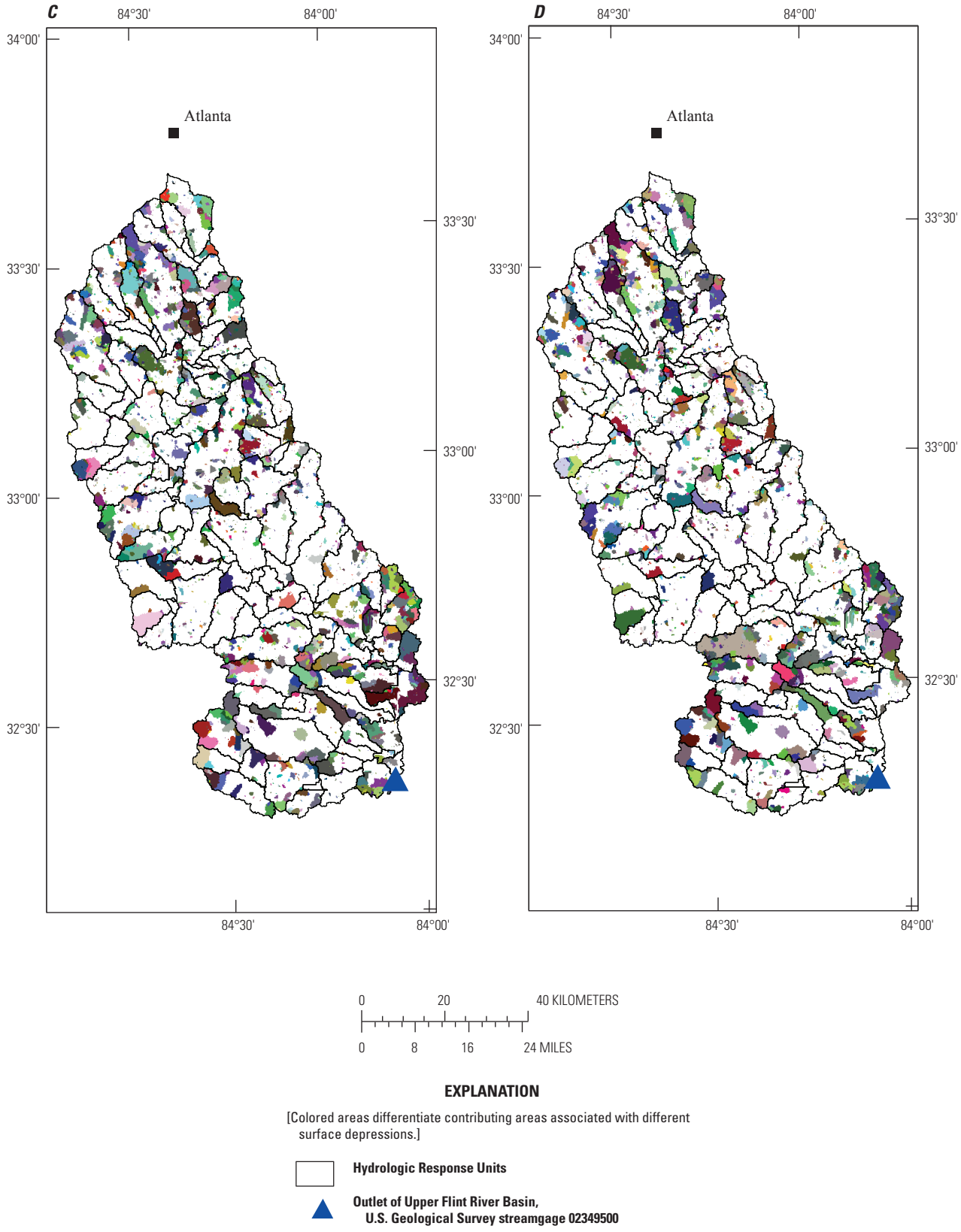

Figure 8. Contributing areas to surface depressions were defined: (*A*) using entirety of surface depressions; (*B*) using nonstream parts of surface depressions; (*C*) using only parts of surface depressions that are at least 300 meters from the streams; and (*D*) using only surface depressions that are entirely 300 meters from streams (that is, if any part of a surface depression is within 300 meters, it is excluded).—Continued

For this study, imperviousness was derived by using the National Land Cover Database (NLCD) 2001 imperviousness dataset (Yang and others, 2003; Homer and others, 2004; Homer and others, 2007), which has a 30-meter cell size and is based on imagery acquired in 2001. Cells with values exceeding 0.05 percent in the NLCD imperviousness data set were set to a value of 1.0 in a derivative raster data set. All other cells were set to null values in the derivative set. This threshold was selected because it clearly demarcated roads and other developed land surfaces that PRMS normally treats as impervious.

Table 3 shows the per-NLCD class statistics for imperviousness. Although the chosen threshold is much lower than the mean values for any of the developed land-cover categories, this threshold ensures that urban areas and paved roads were identified as impervious. Nondeveloped areas show average imperviousness values below this threshold. Figure 9 shows the spatial pattern of the derived impervious surfaces with the HRU boundaries superimposed. The extensive impervious area at the north end of the basin is the city of Atlanta, Ga.

For this study, the area of binary imperviousness was not tabulated for each HRU. The term, binary imperviousness, refers to how PRMS conceptualizes imperviousness. PRMS considers a land surface as completely impervious (like a rooftop or parking lot) or completely pervious (like sand, offering resistance to infiltration only as a function of soil-moisture content). Instead, only binary impervious areas that were not upslope (that is, within the contributing areas) from surface depressions were used to calculated **hru_percent_imperv**. Figure 10 shows the results of this filtering process as effective impervious area. At the scale of the entire basin, one may be able to detect some differences from the image in figure 9. Figure 10*B* shows an enlargement of the northern part of the basin, at the edge of the city of Atlanta, where it is more apparent that the portions of the binary imperviousness map have been excluded on the basis of the contributing areas to surface depressions (which are defined in figure 8*D*). Table 4 shows basinwide statistics of per-HRU imperviousness calculated by using the binary and the effective approaches.

HRU Soil Zone Outflow Concepts and Parameter Preparation

Each HRU soil zone has a capacity to hold water. Once this capacity is filled, runoff is generated. Water can move from the HRU soil zone to the atmosphere either through evaporation or transpiration. In addition, water can leave this zone and move to other HRU soil zones or to two other types of below-ground components. These other types are the subsurface reservoirs and the groundwater reservoirs within the basin, referred to by the model as **nssr** and **ngw**, respectively.

Water can move from a subsurface reservoir to another subsurface reservoir, to the stream, or to a groundwater reservoir. Moisture can move from a groundwater reservoir to another groundwater reservoir, to a stream, or to a sink. Although figure 4 provides a convenient overview of the components and vertical fluxes within the model, it does not show all lateral fluxes between HRUs, subsurface reservoirs, and groundwater reservoirs. The types of fluxes and the parameters that control them are defined as a result of the user's selection of a routing mechanism for the particular application of the model.

The parameters used to characterize these below-ground fluxes are defined below, in table 5, and in (Leavesley and others, 1983). In PRMS, fluxes are expressed as a depth of water over a unit of area, a volume. The volume is expressed per time step (in other words, divided by the time step). These 'volumes'

Table 3. Statistics of urban impervious percentage per National Land Cover Database 2001 land cover categories within the Flint River Basin.

National Land Cover Database 2001 land cover	Minimum	Maximum	Mean	Standard deviation	Median
Open water	0	100	0.0167	0.9011	0
Developed, open space	0	98	8.1069	6.8448	6
Developed, low intensity	0	100	30.0042	10.6924	29
Developed, medium intensity	0	100	60.9630	14.2019	62
Developed, high intensity	0	100	90.5925	12.7791	94
Barren land, rock, sand, clay	0	100	.2862	3.8011	0
Deciduous forest	0	100	.0228	.6542	0
Evergreen forest	0	94	.0239	.7712	0
Mixed forest	0	70	.0277	.7761	0
Shrub, scrub	0	64	.0069	.3896	0
Grassland, herbaceous	0	93	.0217	.7259	0
Pasture, hay	0	100	.0410	1.2026	0
Cultivated crops	0	100	.0319	1.1126	0
Woody wetlands	0	41	.0012	.1469	0

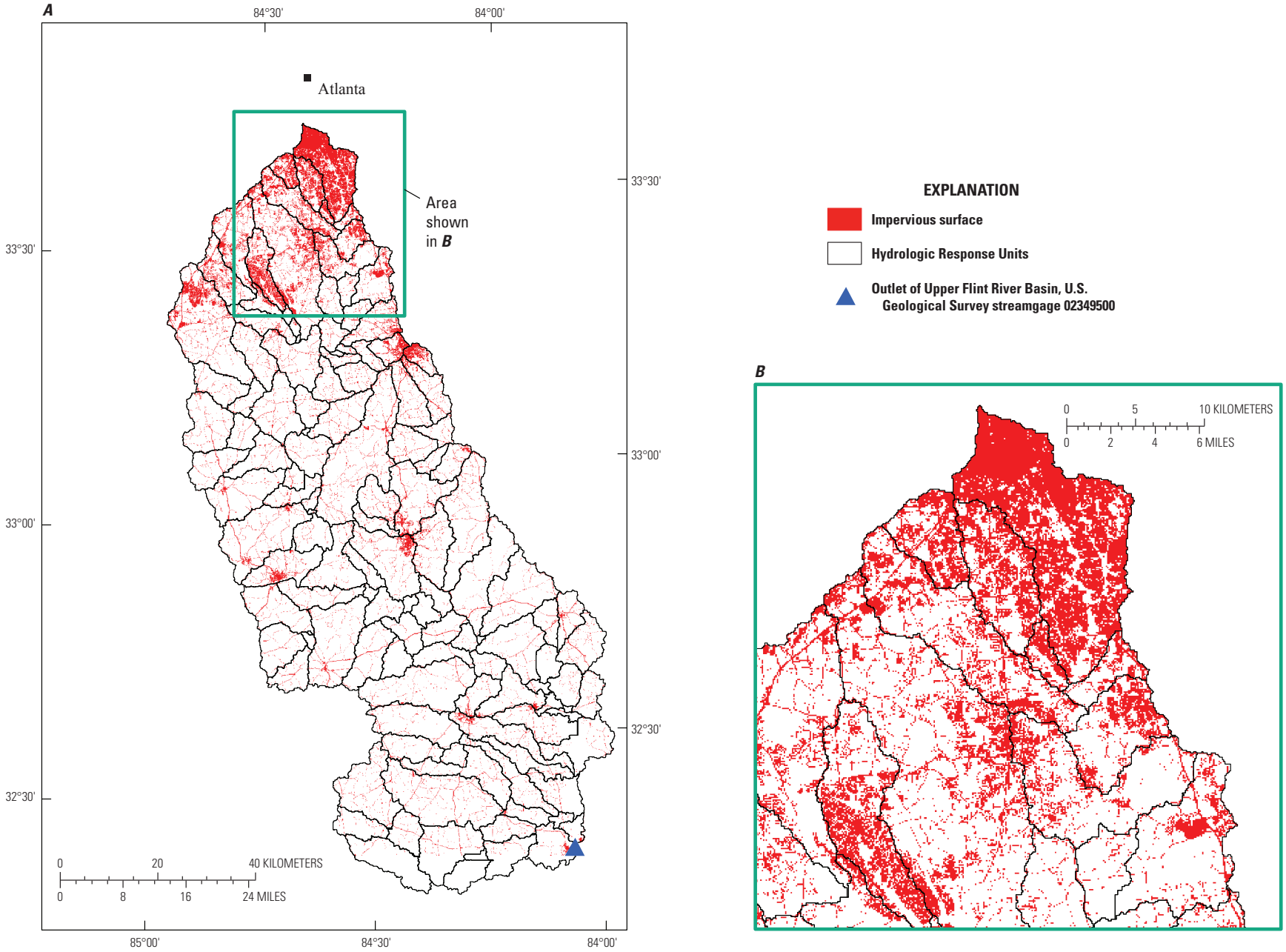

Figure 9. National Land Cover Database Urban Impervious areas exceeding a 0.5 percent imperviousness threshold for: (*A*) the entire Upper Flint River Basin; and (*B*) an enlargement of the area in the green box in (*A*), near Atlanta.

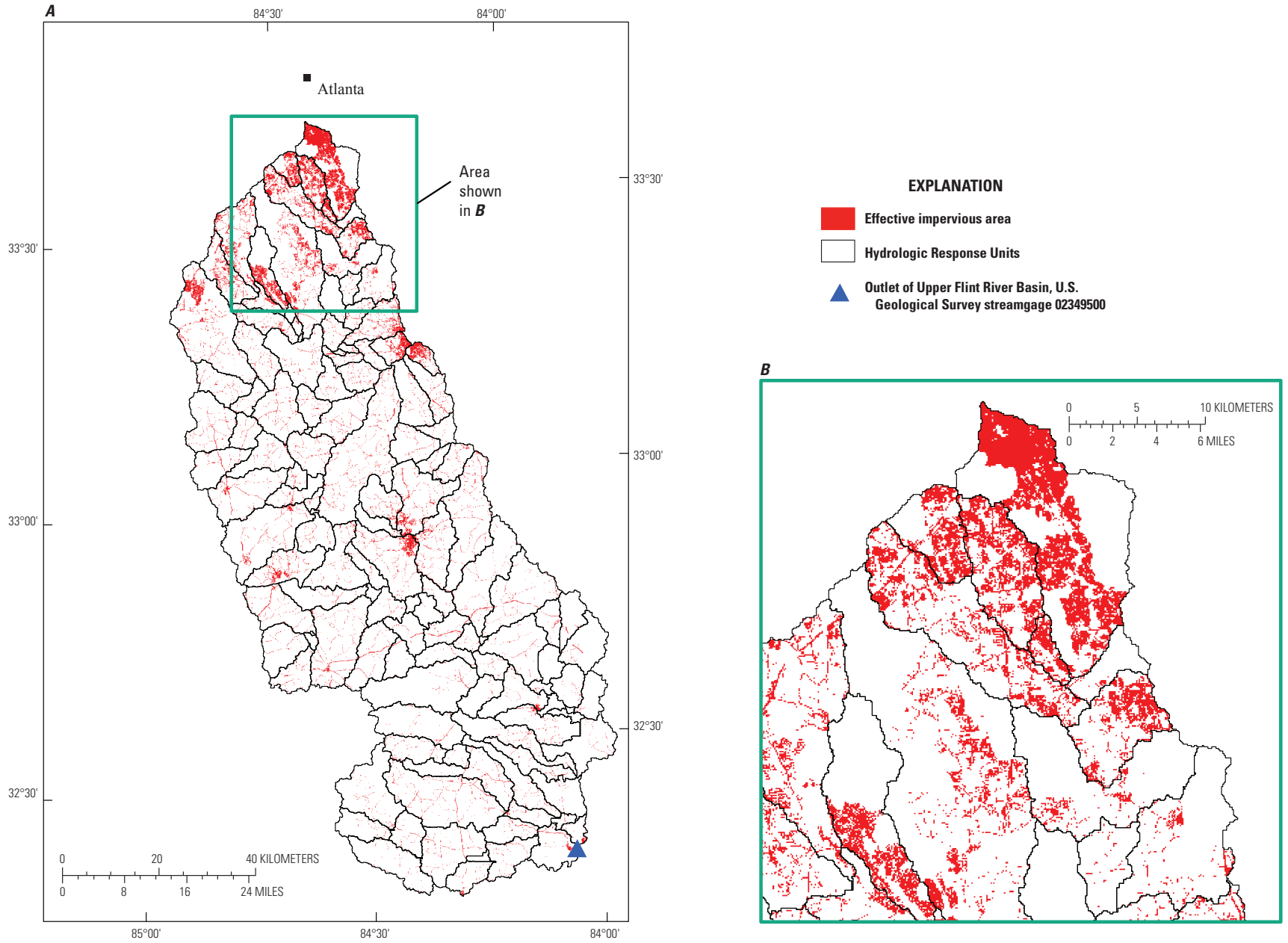

Figure 10. Effective impervious areas, shown in red, not draining to a surface depression for: (*A*) the entire Upper Flint River Basin; and (*B*) an enlargement of the area in the green box, near Atlanta.

are expressed in inches; inches associated with a given flux parameter value is an indication of the volume of water that can pass in a time step.

soil2gw_max Water in excess of the HRU soil-water capacity flows to the groundwater reservoirs. This parameter, expressed in inches, is the maximum amount, or flux, of excess soil water that can be routed to the groundwater reservoir associated with the HRU. This flux can be thought of as the maximum daily recharge of a groundwater reservoir from an HRU soil zone.

ssr2gw_exp A nonlinear coefficient used to route water from the subsurface reservoirs to the groundwater reservoirs, unitless.

ssr2gw_rate A linear coefficient in the equation used to route water from the subsurface reservoirs to the groundwater reservoirs, expressed 1/day.

fastcoef_lin A linear coefficient to route preferential-flow storage from the HRU soil zone downslope according to the selected routing scheme. It is expressed in 1/day (or the functionally equivalent day – 1).

fastcoef_sq A nonlinear coefficient to route preferential-flow storage from the HRU soil zone downslope according to the selected routing scheme. It is unitless.

ssstor_init The storage of water in each subsurface reservoir at the first time step of the simulation period, expressed in inches.

gwstor_init The storage of water in each groundwater reservoir at the first time step of the simulation period, expressed in inches.

gwflow_coef The routing coefficient controlling the speed of flow between each groundwater reservoir and the associated stream segment, expressed in 1/day.

Table 4. Statistics of average Hydrologic Response Unit percent impervious surface based on the binary and effective approaches.

Statistic	Binary imperviousness	Effective imperviousness
Minimum	0.004842	0.000878
Maximum	.766696	.536737
Mean	.087770	.058996
Standard deviation	.123105	.093399

Table 5. Precipitation-Runoff Modeling System parameters defined using hydrogeological groupings.

Precipitation-Runoff Modeling System parameter	Description	Units	Default range
soil2gw_max	The maximum amount of the soil water excess for an Hydrologic Response Unit that is routed directly to the associated groundwater reservoir each day.	inches	0–5
ssr2gw_exp	Nonlinear coefficient used to route water from the subsurface reservoirs to the groundwater reservoirs.	unitless	0–3
ssr2gw_rate	Linear coefficient in equation used to route water from the subsurface reservoirs to the groundwater reservoirs.	1/day	0–1
fastcoef_lin	Linear coefficient to route preferential-flow storage from the Hydrologic Response Unit soil zone downslope according to the selected routing scheme using the following equation: **pref_flow** = **fastcoef_lin** * **pref_flow_stor** + **fastcoef_sq** * **pref_flow_stor****2, where **pref_flow_stor** is soil storage based on preferential-flow pore density and **pref_flow** is interflow as a result of preferential-flow pore space.	1/day	0–1
fastcoef_sq	Linear coefficient to route preferential-flow storage from the Hydrologic Response Unit soil zone downslope according to the selected routing scheme using the following equation: **pref_flow** = **fastcoef_lin** * **pref_flow_stor** + **fastcoef_sq** * **pref_flow_stor****2,	unitless	0–1
ssstor_init	The storage of water in each subsurface reservoir at the first time step of the simulation period.	inches	0–20
gwstor_init	The storage of water in each groundwater reservoir at the first time step of the simulation period.	inches	0–20
gwflow_coef	The routing coefficient controlling the speed of flow between each groundwater reservoir and the associated stream segment.	1/day	0–1

These parameters control the rate and maximum fluxes out of a given component (HRU soil zone, subsurface reservoirs, and groundwater reservoirs); they do not specify the routing destination of these fluxes. PRMS moves moisture through the basin according to the routing scheme selected by the user. In this study, because the Muskingum routing module was chosen, every HRU is connected to a single stream segment. There is no transmission of water between the soil zones of different HRUs. Each HRU has its own subsurface and groundwater reservoir (the HRU map also is used to represent these feature types). Fluxes out of each subsurface and groundwater reservoir are routed to the same stream segment as the associated HRU. Vertical fluxes between the three components occur normally, regardless of the routing procedure being used.

Traditionally, these flux parameters have been set to default values and calibrated. In this study, the fluxes were defined on the basis of "hydrogeological" groupings (fig. 11) derived from GIS maps of surficial geology. These groupings were used to estimate hydraulic conductivity and permeability values for the soil column associated with each group. The estimates then were used to heuristically define parameters indicating the flux rates between HRUs and the subsurface within the basin. Although the hydraulic conductivity values were estimated in collaboration with hydrogeologic experts, the values were not expected to be highly accurate in absolute terms. The main goal of deriving flux parameters from this information was to determine which HRUs are underlain by relatively more or less conductive soils and geology. The parameter estimation process was based on the expertise of the modelers and not on any algorithm or fixed methodology. It was assumed that the absolute values of the parameters could be resolved through the calibration process as long as the initial parameter estimates showed an accurate spatial pattern across HRUs, in relative terms.

The geologic data set used was originally produced as a paper map by Soller and Reheis (2004) and has been recently published as a digital GIS data set (Soller and others, 2009). The surficial material designations were reclassified into six hydrogeological groups. Table 6 lists the descriptive names and assigned characteristics (Jonathan Caine and Carma San Juan, U.S. Geological Survey, written commun., 2009). The area-weighted average hydraulic conductivity (K) was calculated for each HRU to define the initial values for the parameters listed in table 5. The range in K values for the Upper Flint River Basin was 5E-09 to 1E-03 square meters. Freeze and Cherry (1979) give a range of K values from 1E-14 to 1. Default ranges for the parameters listed in table 5 were scaled on the basis of the K information. The resulting parameter values were thought to have a spatially relevant distribution. Model calibration was used to fine tune the HRU values.

Streamflow Routing

PRMS offers three choices for handling of water within a basin:

1. A no-flow routing option;
2. A cascading-flow routing procedure; and
3. A Muskingum-flow routing procedure.

No-Flow Routing

When modeling a basin, the option of no routing is an appropriate choice when simulated runoff for a given time step arrives at the basin outlet during that time step for any HRU in the basin. This option may not be appropriate in basins where travel time from the headwaters to the basin outlet is greater than the simulation time step. Although this method and an additional option to summarize flow at internal nodes (grouping HRUs into subbasins) are available, they offer no lagging of streamflow. All runoff arrives at the outlet of the basin in the same time step in which it was generated. An analysis of internal streamgages within the Upper Flint River Basin indicated a travel time from the headwaters to the outlet of greater than one day, indicating that the "no-flow" routing option would not be appropriate.

Cascading-Flow Routing

The cascading-flow procedure was developed to route surface and subsurface runoff among HRUs and to streams by using an acyclic-flow network (Ford and Fulkerson, 1956). This option is documented in (Markstrom and others, 2008). Flow paths start at the highest upslope HRUs and continue through downslope HRUs until reaching a stream segment. Cascading flow may occur along many different paths; surface and subsurface flow from one upslope HRU may provide inflow to as many downslope HRUs as is required to conceptualize the basin drainage pattern. The stream network in the Upper Flint River Basin does not require the complexity of the 'cascade' option.

Muskingum-Flow Routing and Parameter Descriptions

For this study, the Muskingum option, referred to as **musroute_prms** within PRMS, was chosen for flow routing within the Upper Flint River Basin. The Muskingum flow routing method is a relatively simple and commonly used hydrologic routing method for handling a variable discharge-storage relation. This option for PRMS is documented in Mastin and Vaccaro (2002).

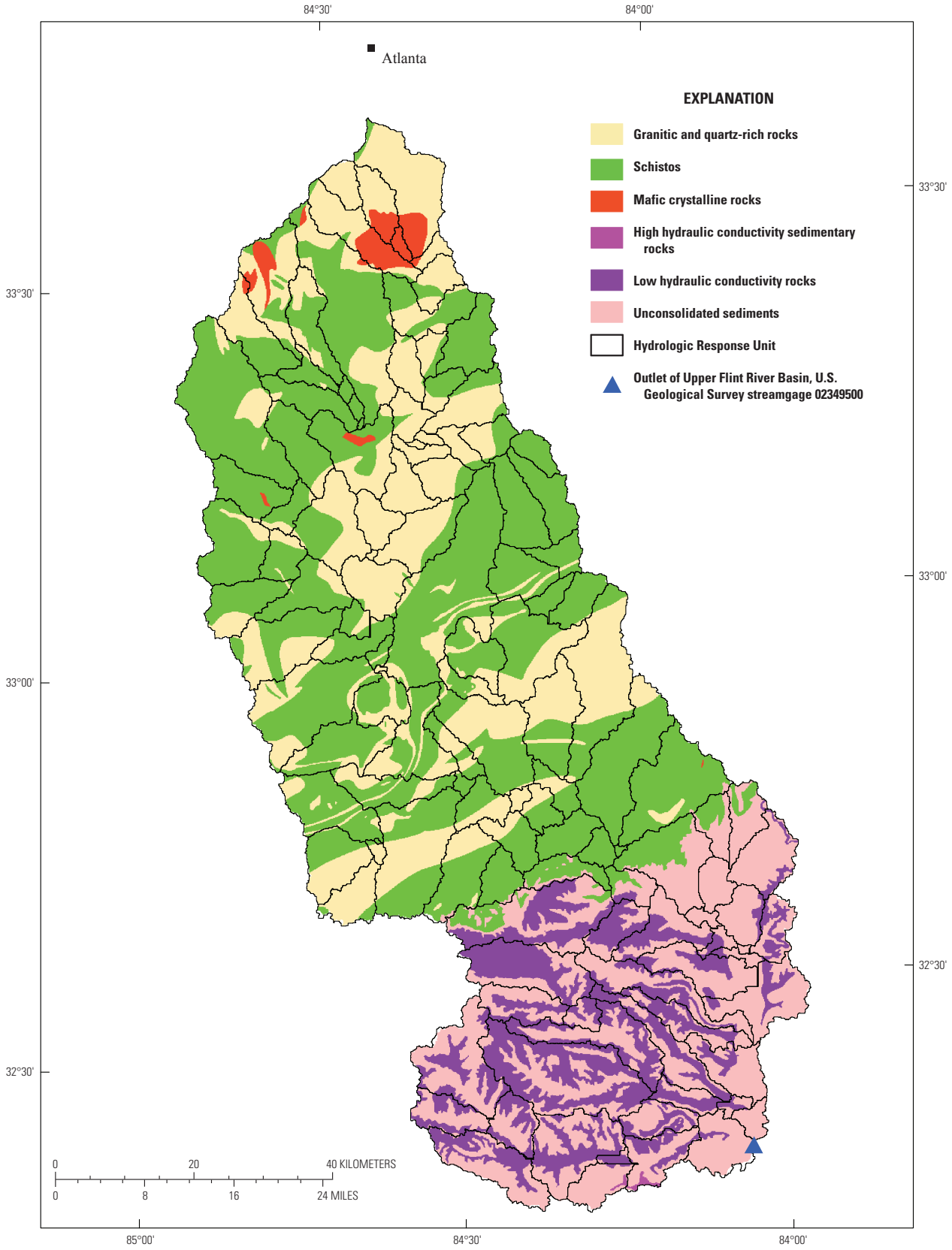

Figure 11. Hydrogeologic groups in the Upper Flint River Basin.

Table 6. Hydrogeological groupings used to assign below-ground flux rates.

Hydrogeological group	Description	Relative hydraulic conductivity	Mean hydraulic conductivity (meters per second)	Mean soil permeability (square meters)
1	Granitic and quartz-rich rocks	4	5.00E-08	5.00E-15
2	Schistos rocks	6	5.00E-09	5.00E-16
3	Mafic crystalline rocks	5	1.00E-08	1.00E-15
4	High hydraulic conductivity sedimentary rocks	2	5.00E-07	5.00E-14
5	Low hydraulic conductivity sedimentary rocks	7	1.00E-09	1.00E-16
6	Unconsolidated sediments	1	1.00E-03	1.00E-10

Four parameters are needed for the Muskingum-flow routing:

K_coef, **x_coef**, **tosegment**, and **hru_segment** These parameters, described below, were derived by using a plug-in to the GIS Weasel (Viger and Leavesley, 2007). The software used to derive the Muskingum parameters is available from the GIS Weasel development team (http://www.brr.cr.usgs.gov/weasel, accessed November 21, 2009), in the form of the "musroute_prms" plug-in.

K_coef The travel time through each stream segment (roughly analogous to travel time in hours). The value of the **K_coef** parameter is derived on the basis of assumptions about the hydraulic radius and bed roughness of a stream segment as a function of its Shreve stream order (Shreve, 1966). The segment slope and length also are considered when deriving the **K_coef** parameter.

The **K_coef** is calculated for each stream segment by multiplying the segment length by an estimated velocity of flow within the length. Velocity is calculated according to Manning's equation (Bedient and Huber, 1988, equation 4.30):

$$V = slope\ 0.5 * radius\ (2/3) * 1.49 / n\ , \qquad (3)$$

where *slope* is the segment slope, *radius* is the cross-sectional radius of the segment, and n is the stream order of the segment. The $radius^{(2/3)} * 1.49 / n$ portion of the equation is referred to here as a *velocity coefficient*. Because no information about the cross-sectional radius of the segment was available, the authors assumed a radius on the basis of the stream order, *n*. The stream order was calculated according to Shreve (1966); headwater segments were considered first order and the stream order increased by the segment downslope of every confluence. Velocity coefficients were set at 12.89, 30.23, 30.23, and 67.31 for first-, second-, third-, fourth- and higher order streams, respectively, on the basis of the authors' survey of literature regarding the morphology and roughness of streams as a function of stream order. An important factor of this approach, beyond the absolute value of the coefficients assigned per-stream order, is the density of the GIS map used to represent the network of stream segments.

Figure 5 shows the results of the previously defined methodology when it was applied to the Upper Flint River Basin. Figure 5 colorizes each segment on the basis of the accumulated **K_coef** values between the segment and the outlet, roughly indicating the number of hours it takes water in that segment to leave the basin. The largest accumulated **K_coef** is just under 40. Streamflow-data analysis in the Upper Flint River Basin gave estimates of maximum travel time at approximately 2.5 days (60 hours).

x_coef A relative weighting of inflow and outflow to a stream segment used to determine storage (Bedient and Huber, 1988). The **x_coef** parameter was set to a default value of 0.25 for all segments and was calibrated.

tosegment The downstream segment that receives flow for each stream segment. The user needs to ensure that the sequence in which the stream segment identification numbers are ordered is such that they increase in the downstream direction. In addition, the highest stream segment identification number needs to equal the number of streams in the network. If there are three stream segments in the network, then the set of identification numbers should be 1, 2, 3, with 1 and 2 flowing into 3. A segment can only drain to one other segment (that is, there can be no divergence of flow). The values were derived by using standard DEM-based analyses of the flow direction (Jenson and Domingue, 1988) of stream segments (Viger and Leavesley, 2007).

hru_segment The downstream segment that the runoff from an HRU drains into. An HRU can only drain to one segment. An HRU cannot drain to another HRU in this routing scheme. The values were derived by using standard DEM-based analyses of the adjacency of HRUs and stream segments (Viger and Leavesley, 2007).

Precipitation-Runoff Modeling System Input Data Sets

For each HRU, PRMS requires daily inputs of precipitation and maximum and minimum air temperature. Precipitation and the form of the precipitation (rain, snow, or a mixture of both) is important to the simulation of snow accumulation, snowmelt, infiltration, and runoff. Precipitation form on each HRU can be specified or it can be estimated from the HRU maximum and minimum daily air temperatures and their relation to temperature when precipitation is all snow. Air temperature is used in computations of evaporation, transpiration, sublimation, and snowmelt for each HRU. PRMS has a selection of modules that can compute and distribute precipitation and temperature for each HRU for each daily time step on the basis of observations at stations.

The **xyz_dist** methodology was chosen to distribute precipitation and temperature data within the PRMS model for the Upper Flint River Basin. This uses a three-dimensional multiple-linear regression, on the basis of longitude (x), latitude (y), and altitude (z), to distribute temperature and precipitation station data to HRUs (Hay and Clark, 2000; Hay and Clark, 2003). The methodology was initially developed to distribute statistically downscaled precipitation and temperature from an atmospheric model (a single grid point) to each HRU in a basin (Hay and Clark, 2000). Further testing of the methodology found it appropriate for distributing station data as well (Hay and Clark, 2000; Hay and others, 2002; Hay and McCabe, 2002; Hay and others, 2006a; Hay and others, 2006b; Hay and others, 2006c). For further details on this module, see the associated web page at http://wwwbrr.cr.usgs.gov/projects/SW_MoWS/software/oui_and_mms_s/ prms_files/xyz_dist.shtml (accessed November 21, 2009).

General Procedure for Calibration of the Precipitation-Runoff Modeling System

The PRMS model was calibrated by using the Luca software (Hay and Umemoto, 2006) to carry out a multiple-objective, step-wise, automated calibration procedure similar to that outlined in Hay and others (2006c). The procedure used the Shuffle Complex Evolution global search algorithm (Duan and others, 1992; Duan and others, 1993; Duan and others, 1994) to calibrate PRMS in the Upper Flint River Basin of Georgia. For this study, four steps were used in the calibration procedure. Table 7 lists the sequence of calibration steps and associated calibration data set, objective function(s), and model parameter(s). For each of the four calibration steps, the following calibration data set was developed to compare with PRMS outputs:

1. Basin mean monthly solar radiation (SR);
2. Basin mean monthly potential evapotranspiration (PET);
3. Water-balance configurations; and
4. Daily runoff components of flow. This process ensures that intermediate states of the model (SR and PET on a monthly mean basis), as well as the water balance and components of the daily hydrograph, are simulated consistently with observed values.

Details of Precipitation-Runoff Modeling System Calibration in the Upper Flint River Basin

The multiple-objective, step-wise, automated procedure described above was used to calibrate the hydrologic model PRMS in the Upper Flint River Basin. USGS streamgage 02349500 at Montezuma, Georgia, was used for model calibration. This streamgage has reliable record from July 1930 through September 2003 (U.S. Geological Survey National Water Information System, 2009). For this study, a split sample test was used for calibration and evaluation of PRMS. Ten water years (WYs) 1990–1999 were chosen for model calibration. Fourteen WYs, 1980–1989 and 2000–2003, were chosen for model evaluation.

Four hydrologic-model outputs were calibrated:

1. Monthly mean SR;
2. Monthly mean PET;
3. Annual water balance components; and
4. Daily runoff components.

Four rounds of the step-wise calibration procedure were needed to reach a minimum in each objective function tested.

Solar Radiation (SR) Calibration of SR is the first step in the step-wise procedure. Figure 12 shows the basin mean monthly SR values for observed (gray line), calibrated (blue line), and evaluated (green line) SR values. The calibrated values (WYs 1990–1999) are most similar to those shown for observed SR. The evaluated values (WYs 1980–1989 and 2000–2003) show close agreement with observed values, with small exception in June and August.

Potential Evapotranspiration (PET) Calibration of PET is the second step in the step-wise procedure. Figure 13 shows the basin mean monthly PET values for observed (gray line), calibrated (blue line), and evaluated (gray line) PET values. Results for PET are similar to those shown for SR. The temperature differences between the calibration and evaluation periods in June and August (not shown) directly affect the PRMS-simulated SR and PET in those months.

Table 7. Calibration procedure.

Calibration data set (model state)	Objective unction(s)	Parameters used to calibrate model state	Parameter range		Parameter description
		Calibration step 1			
Basin mean monthly solar radiation	Absolute difference	**dday_intcp**	–60.0	10.0	Intercept in temperature degree-day relation
		dday_slope	.2	.9	Slope in temperature degree-day relation
		tmax_index	50.0	90.0	Index temperature used to determine precipitation adjustments to solar radiation, units specified by **tmax_index** parameter
		Calibration step 2			
Basin mean monthly potential evapo-transpiration (PET)	Absolute difference	**jh_coef**	.005	.09	Coefficient used in Jensen-Haise PET computations
		Calibration step 3			
Water balance	Normalized root mean square error: 1. Annual 2. Monthly mean 3. Mean monthly	**adjust_rain**	–1.0	1.0	Precipitation adjustment factor for rain days
		psta_nuse	0	1	Binary indicator for using station in precipitation distribution calculations
		psta_freq_nuse	0	1	Binary indicator for using station in precipitation frequency calculations
		Calibration step 4			
Daily streamflow	Normalized root mean square error: 1. Daily	**dprst_flow_coef**	.0001	3	Coefficient in depression flow routing computations
		dprst_seep_rate	.0001	1	Coefficient in depressions seepage flow computations
		fastcoef_lin	0	1	Linear preferential-flow routing coefficient
		fastcoef_sq	0	1	Non-linear preferential-flow routing coefficient
		gwflow_coef	.001	.05	Groundwater routing coefficient
		K_coef	0	48	Travel time through stream segment, hours
		op_flow_thres	0	1	Percent of maximum open surface depression storage above which flow occurs
		smidx_coef	1.0E-4	1.0	Coefficient in nonlinear surface runoff contributing area algorithm
		smidx_exp	.2	.8	Exponent in nonlinear surface runoff contribution area algorithm
		soil_moist_max	0	20	Maximum available water holding capacity of soil profile, inches
		soil_rechr_max	0	20	Maximum available water holding capacity for soil recharge zone, inches
		soil2gw_max	1.0E-4	.5	Maximum rate of soil water excess moving to groundwater, inches

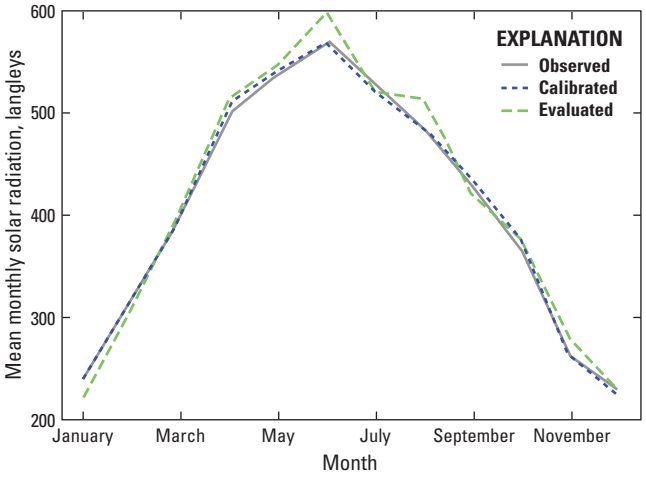

Figure 12. Basin mean monthly solar radiation: observed, calibrated (water years 1990–99), and evaluated (water years 1980–89 and 2000–03).

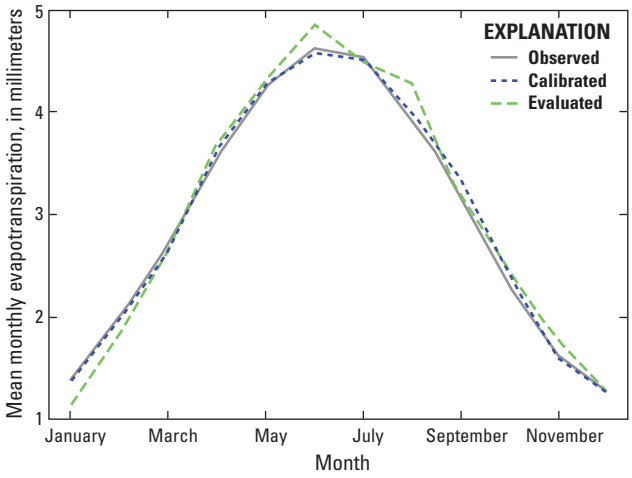

Figure 13. Basin mean monthly potential evapotranspiration (PET): observed, calibrated (water years 1990–99) and evaluated (water years 1980–89 and 2000–03).

Water Balance Calibration of the water balance is the third step in the step-wise procedure. The water balance was calibrated by using the sum of four objective functions, which examined three water-balance categories:

1. Annual water balance;
2. Monthly mean water balance (that is, one value for every month in the period of record); and
3. Mean monthly water balance (that is, 12 values, one for each month of the year).

Figure 14 shows the observed (gray line) daily flow and the simulated daily flow for the calibration period (blue line) and evaluation period (green line) for the (*A*) annual mean, (*B*) monthly mean; (*C*) mean monthly during the calibration period; and (*D*) mean monthly during the evaluation period. In general, observed and simulated water balances show good agreement.

Daily Runoff Calibration of the daily runoff is the fourth and final step in the step-wise procedure. Figure 15*A* shows the observed compared to simulated daily flow values for the calibration period (blue dots) and evaluation period (green dots). Visual inspection of the daily plots shows a good one-to-one fit between observed and simulated values.

The Nash-Sutcliffe goodness of fit (NS) was chosen to evaluate the performance of the PRMS calibration. The NS value is calculated as follows (Nash and Sutcliffe, 1970):

$$NS = 1.0 - \sum_{n=1}^{ndays} (MSD_n - SIM_n)^2 \; / \; \sum_{n=1}^{ndays} (MSD_n - MN)^2, \qquad (4)$$

where MSD are the observed daily runoff values, SIM are the simulated daily runoff values, MN is the average of the observed values, and n is the number of values out of a total of n days (ndays). An NS value of one indicates a perfect fit between observed and simulated. A value of zero indicates that the fit is as good as using the average value of all the observed data.

Figure 15*B* shows the yearly NS statistic values by water year. Figure 15*C* shows the yearly NS statistic values sorted by annual flow volumes (blue dots indicate calibration period, green dots indicate evaluation period, and number indicates WY). The NS results in figure 15 show a high variability in the yearly NS values (0.23–0.85). When sorted by flow volume it becomes evident that the model accuracy increases with annual flow volume, with the exception of WY 2003.

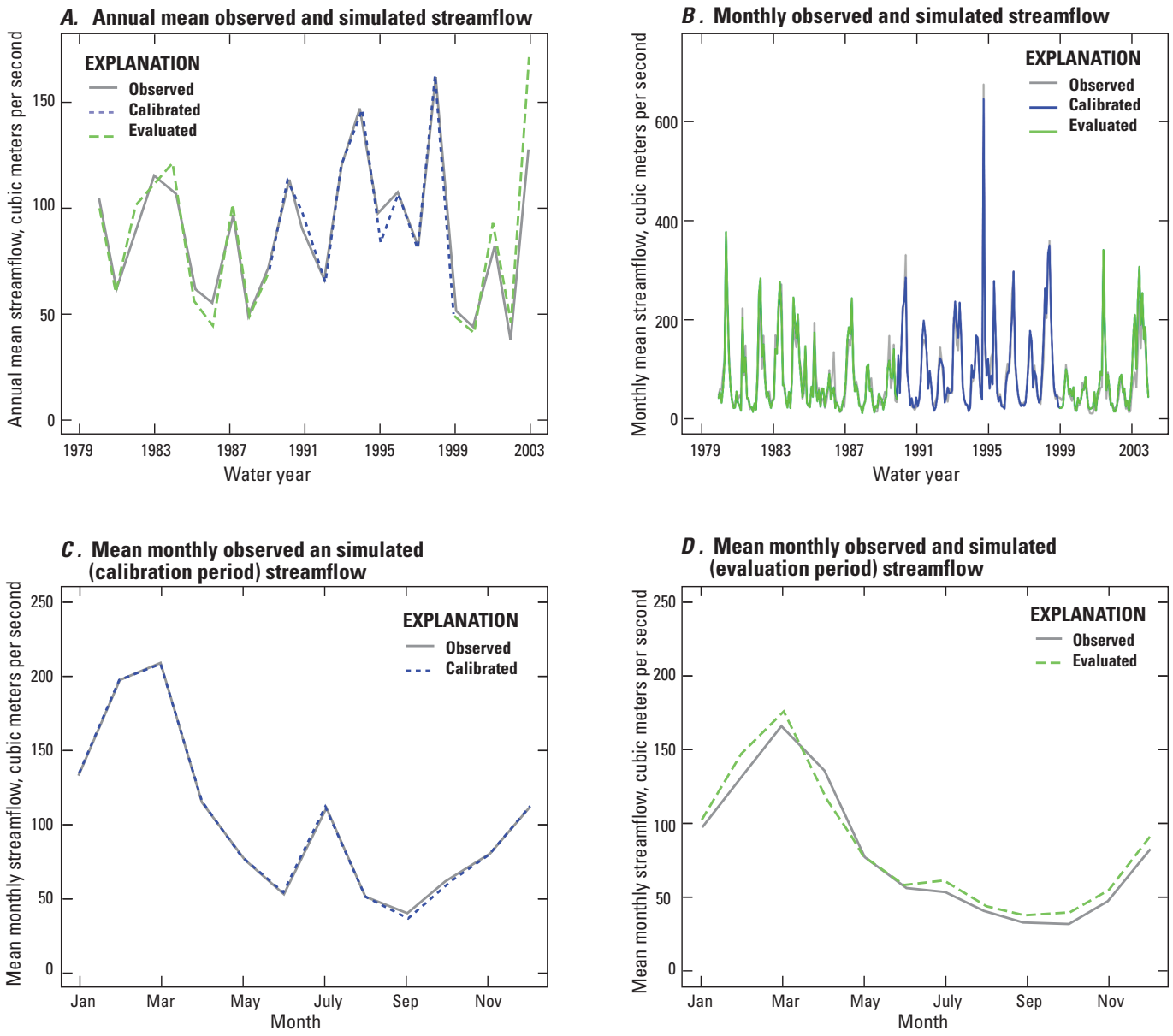

Figure 14. Streamflow water balance results for: (*A*) annual mean; (*B*) monthly mean; (*C*) mean monthly during the calibration period; and (*D*) mean monthly during the evaluation period.

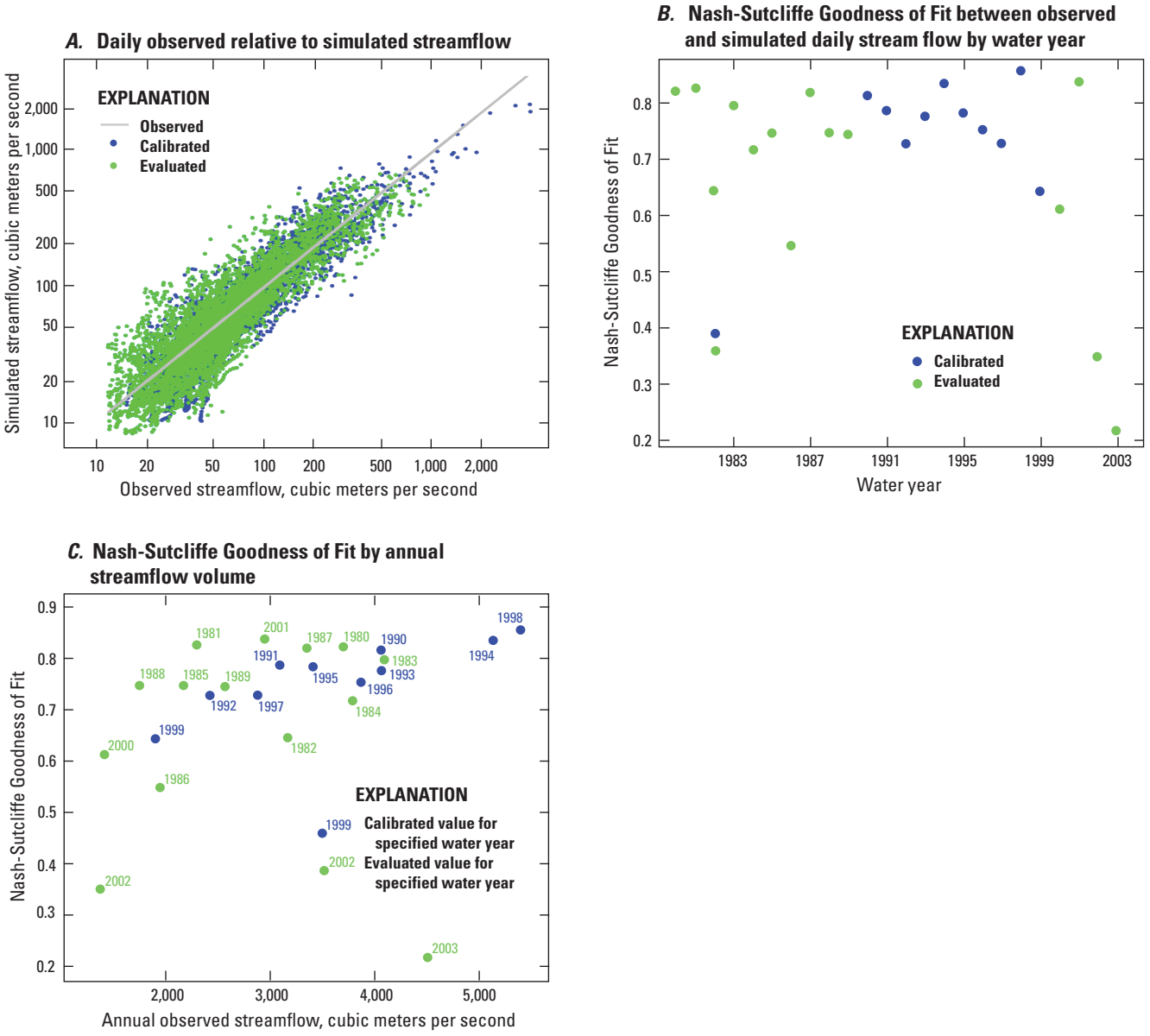

Figure 15. Comparison of observed and simulated daily streamflow: (*A*) observed compared to measured streamflow; (*B*) Nash-Sutcliffe goodness of fit statistic by year; and (*C*) Nash-Sutcliffe goodness of fit statistic by annual streamflow volume.

Effects of Including Surface Depressions in Modeling Process

There are several important effects of the procedures used to generate inputs to the simulation of surface-depression water storage. These are associated with the delineation of the water-body surface areas, estimation of the volumes of the depressions, and the effect these have on streamflow simulations.

Comparison of Surface-Depression Maps

Because this study was unable to verify the ETM+-derived surface-depression delineations with field data, the results of this analysis were evaluated three different ways:

1. Statistics of surface-depression areas derived from ETM+ imagery were compared to those of water bodies designated by the high-resolution version National Hydrography Dataset (NHD) (Simley, 2008),
2. The two delineations (ETM+ and NHD) were overlain to give a more detailed measure of spatial collocation, and
3. Another overlay analysis was carried out by using the ETM+-derived results with those extracted from the DEM data.

Enhanced Thematic Mapper Plus and National Hydrography Dataset Map Statistics

The total area of the 25,498 discrete features derived from ETM+ imagery was 96.5200 square kilometers. The average size of these water bodies was 0.0037 square kilometers, with a standard deviation of 0.03210. The largest ETM+-derived surface depression was 3.12 square kilometers. In comparison, NHD enumerated a total of 6,236 separate water bodies that collectively covered 223.809 square kilometers, with an average area of 0.0358 square kilometers and a standard deviation in size of 0.4023 square kilometers. Within the NHD set of water bodies, there were 5,457 lakes and ponds with an aggregate area of 73.2690 square kilometers and 740 uniquely identified wetlands with an aggregate area of 150.2730 square kilometers. The largest NHD-designated water body was 24.5050 square kilometers. The area of the ETM+-derived surface depressions seems to correspond most closely with the lake and pond features of the NHD. There was almost no overlap of ETM+-derived surface depressions with a major (over 65 square kilometers) NHD swamp just north of the basin outlet (Great Swamp, fig. 1), as well as a number of relatively large (> 1 square kilometer) swampy regions in the north of the basin.

Enhanced Thematic Mapper Plus and National Hydrography Dataset Overlay Analysis

For the second analysis, the NHD water bodies were converted to a raster format and intersected with the other maps of surface depressions. The NHD water bodies for the basin are shown in figure 16*A*. Figure 16*B* shows a portion of the intersection of the NHD water bodies with the ETM+-derived surface depressions. This analysis found that 35.5 square kilometers of the ETM+-derived surface depressions coincided with NHD-designated water bodies, representing 36.78 percent of all surface depressions delineated from the ETM+ data. This area represented 15.75 percent of the NHD-designated water bodies. The analysis did not attempt to measure proximity of features from the two data sets and may underestimate the similarity between the two.

The degree to which the individual cells in the raster representation of these two data sets intersect is summarized in figure 17. Figure 17*A* shows the HRUs color coded to indicate the percentage of HRU area that is occupied by ETM+-derived surface depressions. The mean percentage of HRU area occupied by surface depressions was 1.5989. Figure 17*B* shows the HRUs color coded to indicate the percentage of HRU area that is occupied by NHD-designated lake features. The mean percentage of HRU area occupied by NHD water bodies was 5.0018. Several of the HRUs with high percentages of NHD water bodies are part of the large swamp shown in the southern end of figure 16.

Assessment of National Elevation Dataset-Derived Maps

As a third way to assess the quality of the ETM+-derived surface depressions, these maps were compared with delineations of topographic sinks derived from the USGS National Elevation Dataset (NED). The version of NED used was the DEM described for the rest of the study. Topographic sinks were detected by looking for cells in the DEM that had no outbound flow direction [as determined by using the standard D8 flow-direction algorithm (Jenson and Domingue, 1988)]. If there was a contributing area to such a cell, then this area also was counted as part of that topographic sink. The DEM sinks covered only 0.44 percent of the basin area. This analysis was carried out to provide a comparison with the methodology presented in Vining (2002), although the accuracy of DEM-derived topographic sinks is not expected to be high because of a number of the issues discussed in the “Previous Studies” section. Figure 17*C* shows the HRUs color coded to indicate the percentage of HRU area that is occupied by DEM topographic sinks. The mean percentage of HRU area occupied by topographic sinks was 0.6129.

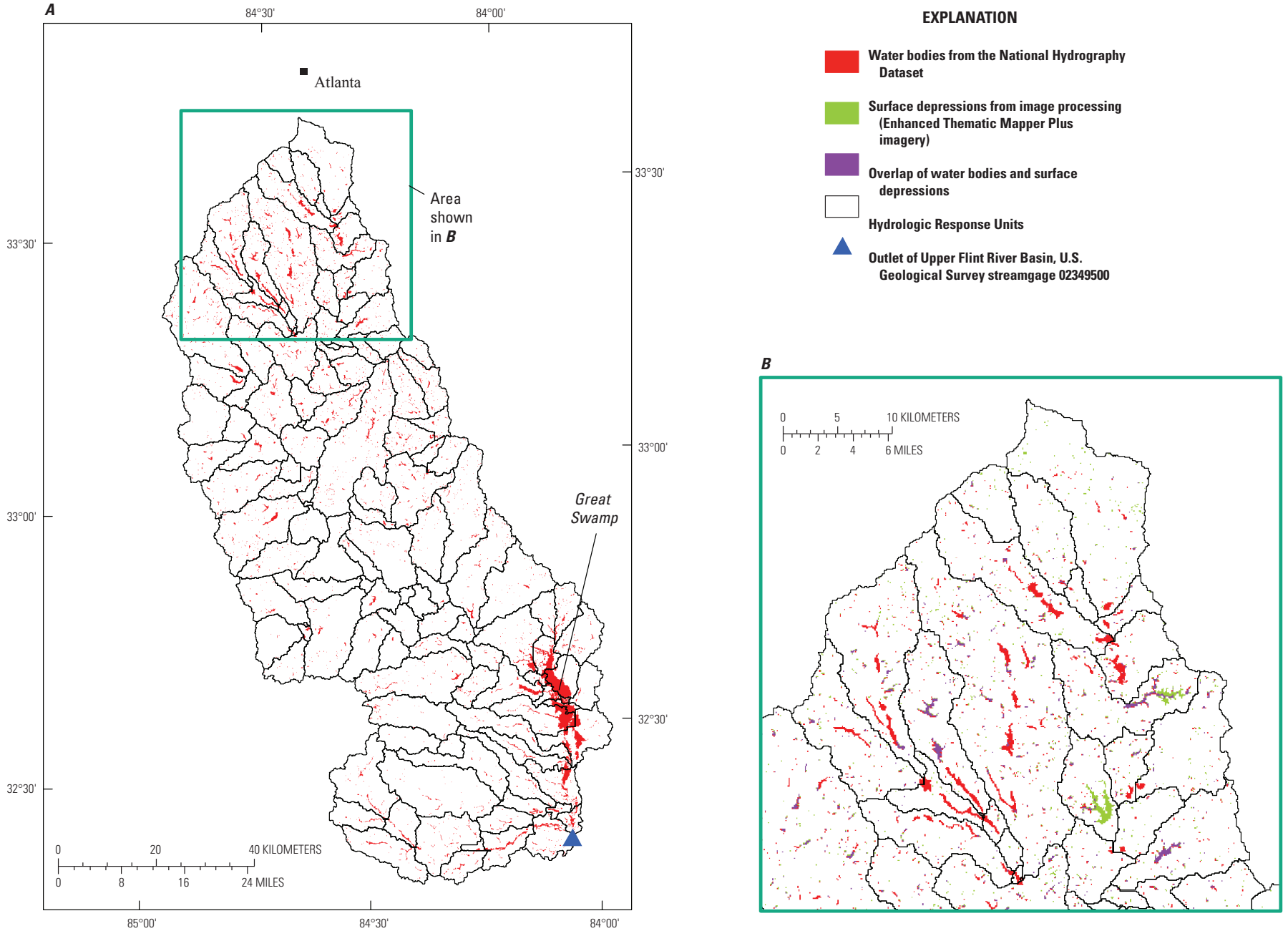

Figure 16. National Hydrography Dataset-designated water bodies are shown: (*A*) for the entire Flint River Basin; and (*B*) for the northern end of the basin indicated by the green box shown in (*A*).

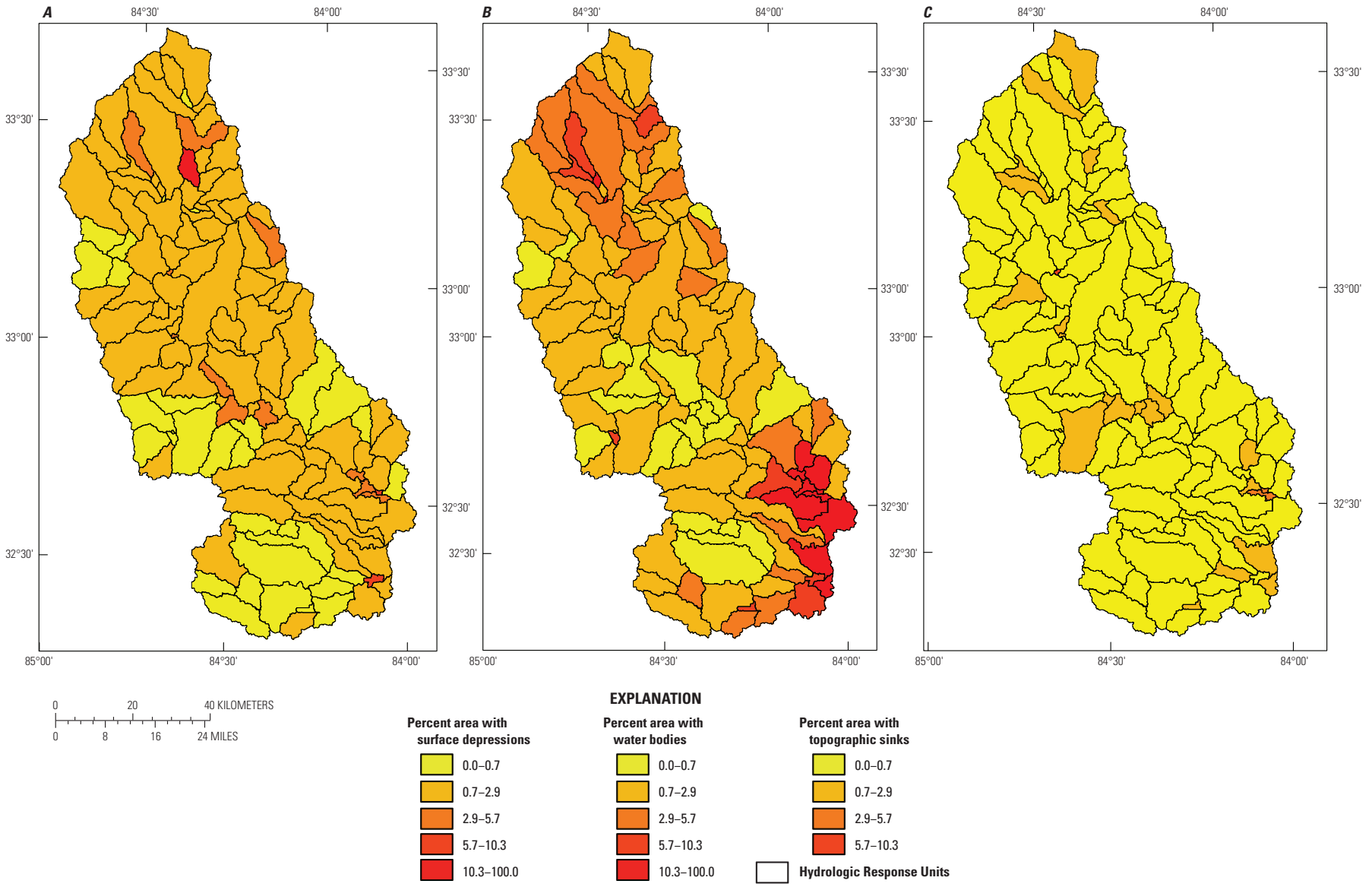

Figure 17. Hydrologic Response Units derived for this study are color coded to indicate the percentage of Hydrologic Response Unit area that is occupied by: (*A*) Enhanced Thematic Mapper Plus-derived surface depressions; (*B*) National Hydrography Database-designated water bodies; and (*C*) digital elevation model-derived sinks.

Figure 18 shows an enlargement of part of the basin area and the relatively strong disagreement between the DEM-derived topographic sinks and the surface depressions derived from ETM+ imagery. The DEM-derived topographic sinks map contains a large number of spurious single-celled surface depressions. In addition, the DEM-derived topographic sink map fails to consistently designate larger ETM+-derived features that resemble rivers and other water bodies. Overlay statistics, calculated to quantify the overlap between the ETM+-derived surface depressions and the DEM-derived topographic sinks, found that 3.92 square kilometers of the ETM+-derived surface depressions coincided with DEM-derived topographic sinks, representing 4.06 percent of the area for all ETM+-derived surface depressions and 11.84 percent of the area for all DEM-derived topographic sinks.

To assess whether the ETM+-derived surface depressions or the DEM-derived topographic sinks more closely approximated the NHD designations, the DEM-derived surface depressions also were overlain with the NHD designations. Although not conclusive, this study found that a DEM-based approach is not adequate. Despite the fact that the agreement between the ETM+ and NHD-based approaches was not very strong, the two data sets were more visually and logically consistent with each other than with the DEM-based results (fig. 17). Differences between ETM+- and NHD-based results can be at least partially explained by differences in their production processing. For instance the NHD process sets a minimum area where the ETM+ process does not. The general morphology of the DEM-based results often appeared to be a function of spurious artifacts in the elevation data created by processing activities, such as projection, that may not be real or hydrologically meaningful.

The most notable difference between the ETM+-derived surface-depression map and the NHD-designated water-body map was the lack of swamps in the former (fig. 16). Future work could use the NHD-designated water bodies (including swamps) to develop the depression storage parameters and enable comparison of model performance with and without swamps. This also could be done by using the topographic sinks in the DEM, even if only to document the (expected) reduced accuracy of using the DEM approach.

On the basis of these analyses, the maps of surface depressions derived from the ETM+ images are considered to be higher quality than those derived from the NED. The ETM+-derived product also is judged to be more helpful than the NHD high-resolution data (the best currently available, 2009) within the context of simulating hydrological processes, because this approach can detect features as small as a single cell within the ETM+ imagery (30 meters across). NHD sets a minimum size threshold of 10 acres (ETM+ cells are less than one-fourth of an acre) for designating a water body. In addition, the NHD high-resolution data are not available at a national scale within the United States or for basins outside the country.

Assessment of Surface-Depression Mapping Procedure

A major strength of this approach is its simplicity. It can be employed by those without a great deal of image processing experience or access to expensive software. However, several points of caution are warranted. First, it is critical that an image date representative of desirable hydrologic and weather conditions is selected. If conditions are too dry, important surface-depression storage capacity will be missed. Second, the selected imagery must be as clear (free of atmospheric effects) as possible over the entire study area. Third, if the entire study area cannot be covered by a single image, the selection of imagery with both similar hydrologic conditions (that is, water levels) and weather conditions may be challenging. If appropriately matched images cannot be found, much more complicated calibration of the various imagery data may be necessary. Finally, as it relies on subjectively set thresholds to extract the surface depressions, operator familiarity with the study area and objective means of output assessment are needed to ensure adequate data quality.

More specifically the quality of the result is dependent on the degree to which the thresholding process mistakenly designates or omits surface-water areas. There was no field verification of the result, although it was compared with the NHD- and NED-based mappings of water bodies. An important aspect of the approach presented here is the establishment of a moisture threshold beyond which the land surface is considered to be holding “standing water” and below which is merely “wet soil.” Another condition that led to misclassification was shading created by trees at the boundary between forest stands and open fields. Users of this technique should look for these and other errors in their application domain.

Evaluation of Surface Area-Volume Regressions

The relation between the surface area and volume of reservoirs derived from the NID database may not be a realistic surrogate for the types of water bodies being considered in this study. By using the NID, the relation was on the basis of reservoirs created by engineered dams. These features typically are much larger than those that are being described by the surface-depression extension of the model; the surface area-volume relation may not be consistent across scales. This is especially likely because the criteria for locating a dam are likely much more stringent than those for the creation of a mill, farm, or storm pond, resulting in erroneously large storage capacity per unit of surface area.

Future work could examine area-volume relations by using the remainder of the NID, with more sophisticated sampling strategies to allow for more statistically rigorous methods to characterize the certainty of the predicted volumes. Although not reported on in detail here, the authors

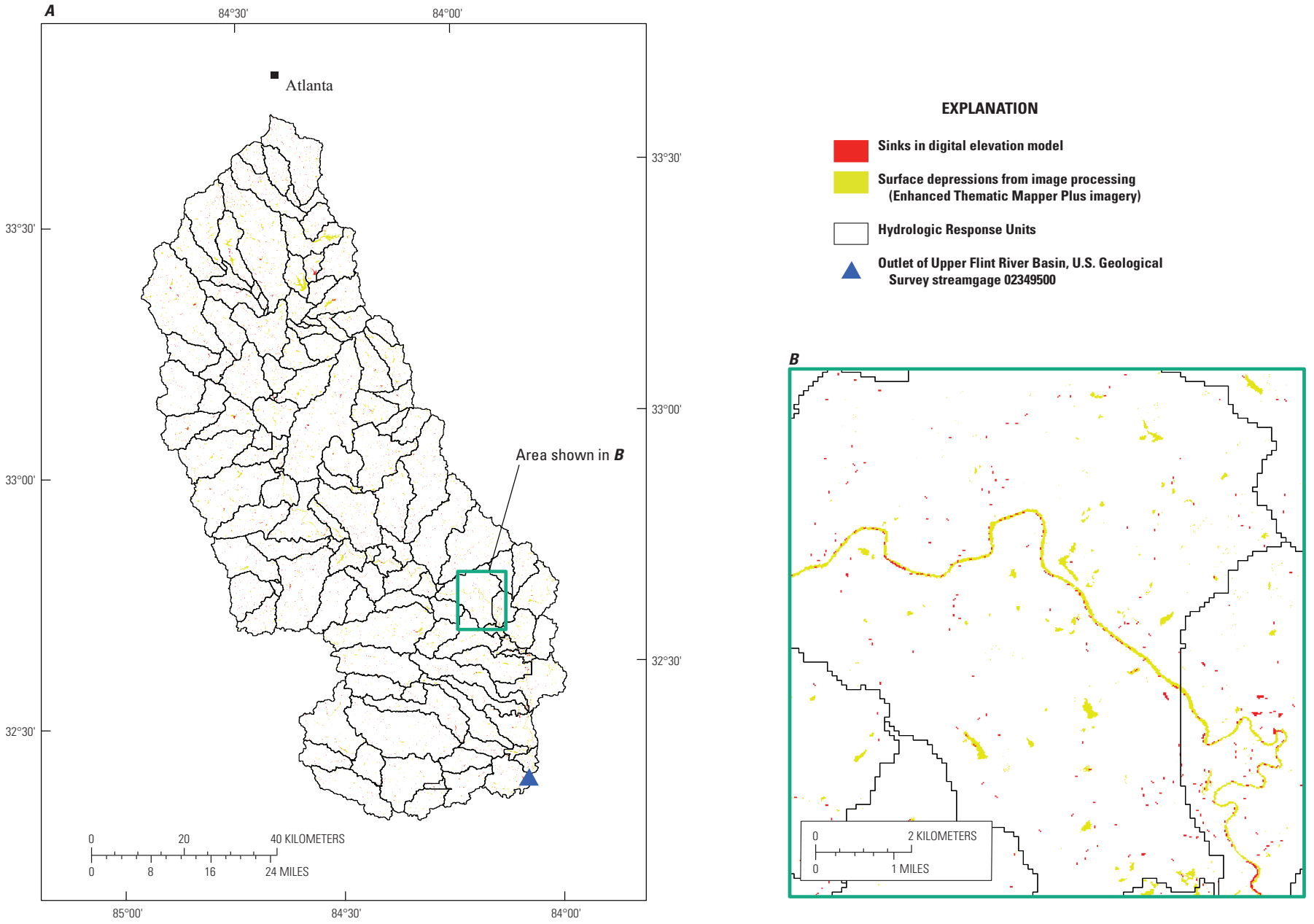

Figure 18. Overlay of topographic sinks extracted from digital elevation model (black) onto Enhanced Thematic Mapper Plus-derived surface depressions (yellow) for: (*A*) the entire Upper Flint River Basin; and (*B*) for smaller area within the basin, outlined in the green box in (*A*).

developed regression equations for subsets of the NID data in the Flint River Basin on the basis of the physiographic region of the water body. The equations for each of the three physiographic regions agreed with the basinwide equation with an R^2 of 0.89 or better. Field measurements, although costly, would be the best way to characterize the relation specifically for surface depressions. In addition, the sensitivity of simulated streamflow to adjustments in storage volume could be more explicitly tested.

Some surface depressions actually were large manmade water bodies, some of which were reservoirs. An important consideration in using the approach for delineation, parameterization, and simulation of surface-depression storage is whether the flows out of these features are actively managed. While most small water bodies simply spill when they are filled, the user needs to understand whether it is accurate to assume that inflows and outflows of all large water bodies are managed or otherwise modified by human activities. If water-body size is an accurate indicator of active flow management, future modeling efforts might assess whether a threshold surface area be used to separate "small" and "large" and use this distinction to designate "unmanaged" and "managed" water bodies.

Effect of Depression Storage on Model Simulations

Figure 19 compares simulated daily streamflow by using PRMS with and without the depression storage parameterization. Including depression storage in the model has the effect of decreasing daily flows for all but the lowest flow values. Conceptually this makes sense; storage ponds are built to mitigate high flows. An advantage of using this module over using other parameters or statistical methods to compensate for depression storage is that it is described as a measurable physical process.

While it may have been possible to provide goodness-of-fit statistics for the streamflows calibrated and simulated without inclusion of the surface depression effects, this would not have yielded meaningful information. The calibration process used (Hay and Umemoto, 2006) is powerful enough to result in goodness-of-fit equal to what was achieved here, but those statistics would fail to recognize whether other hydrological states of the model were simulated accurately. Hay and others (2006c, fig. 11, p. 889) demonstrated this case when they showed that not only their Nash-Sutcliffe values but their annual water balances were excellent, but that the calibration process resulted in substantial errors in the simulation of states other than streamflow, such as solar radiation and potential evapotranspiration.

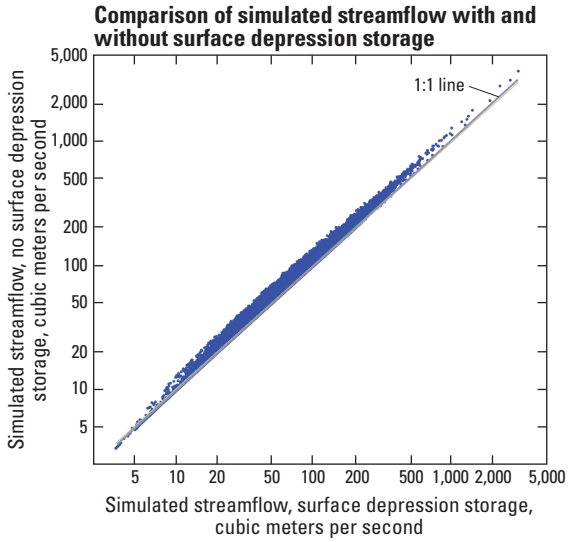

Figure 19. Comparison of daily simulated streamflow with and without depression storage parameterization.

The depression storage parameterization for this example was static but one would envision increased depression storage with increased urbanization. Several enhancements to PRMS could be built to take advantage of the ability to simulate the effect of temporally varying surface depressions. The first notable example is the extension of PRMS to allow "dynamic" parameters that can vary through time (PRMS currently has ≈200 parameters; parameters are static). The concept of dynamic parameters has been previously identified as a way to describe changes to the land cover, including vegetation type and density, during the period of time simulated by the model. Dynamic parameters could be used to describe interactions between depression storage and land cover within an HRU, for example. As an HRU is inundated and storage in surface depressions is increased, grass and shrub types of land cover could be submerged and potentially change the dominant land cover within the HRU.

Further research could be carried out to evaluate whether the approach for simulation of depression storage is valid or necessary for different spatial scales. In addition to referring to basins of differing sizes, this alludes to the resolution of the individual HRUs in the basin. Rather than using the approximately 100 HRUs used for the Flint River Basin, the importance of simulating depression storage also could be tested on the same basin by using only 10, or more than 1,000 HRUs, to describe the same area. Such study could help identify the scale at which the hydrological processes involved in depression-storage units emerge and operate.

Model Limitations

Surface depressions are important to basin modeling because large portions of the United States have hydrologically significant acreages of surface depressions. Although these features might be ignored and the model calibrated to meet some convergence criteria, the model will be producing "the right answer for the wrong reasons." Even then, the "right answer" may only be produced for the calibration period or during previously observed conditions. Properly recognizing this relatively fine-scale geographic feature is important for the development of a scientifically valid national hydrological modeling system and for supporting effective natural resource management. Explicit simulation of water storage in surface depressions could be an important addition to simulations of hydrology in floodplains. This and the other enhancements to the model discussed here and their application provide a more realistic description of basin geography and hydrology that serve to constrain the calibration process to more physically realistic parameter values.

The handling of the imperviousness is particularly important in light of increasing urbanization throughout the Nation. Although an approach for determining effective imperviousness while considering surface depressions is demonstrated and included a detailed discussion of processing choices related to it, direct evaluation of the effect of the changes in parameter values induced by this new approach has not been developed. Research into methods that more effectively exploit the floating-point data content of impervious surface data layers in geographic information systems (GIS) is warranted. The model may need to be reconceptualized to more effectively represent the effect of imperviousness on soil infiltration. Another aspect of the PRMS model implementation to evaluate is whether the idea of surface storage on impervious surfaces (through the **imperv_stor_max** parameter) is redundant to the more explicit simulation of water storage in surface depressions demonstrated in this report.

The methods for describing the hydrologic fluxes between the HRU soil zone, other subsurface reservoirs, and the stream network have the potential to be generalized to use widely available GIS and streamflow data within the United States. While this approach did not change the model itself, it does provide a way to set parameters (to which the model is sensitive), based on observed information. This is an improvement over relying solely on automated calibration procedures that do not incorporate any semantic understanding of the parameters or processes. Although the reclassification of geologic maps to estimate hydraulic conductivity should not be an automatic process, the approach described here clearly defines the needs of PRMS (as wells as other, similar hydrologic models) with regard to characterizing the underground portion of the hydrologic cycle. PRMS does not need detailed geologic description or a wealth of characteristics. Hydraulic conductivity values do not need to be extremely accurate to produce a more realistic simulation of hydrology.

Muskingum routing is demonstrated to be an effective mechanism for accurately simulating the streamflow of the Upper Flint River Basin. The GIS-generated parameters to support the **musroute_prms** module (the HRU-stream and stream-stream connectivity parameters, the **K_coef** parameter) required no adjustment to ensure good temporal matching of simulated with observed peaks in streamflow. This approach is helpful because it enables a model user to quickly and systematically generate this information for large geographic regions where in-stream travel times exceed the daily time step of the model. This mechanism is easy to parameterize and run when contrasted with other more complex approaches (such as those that use cascades or hydraulic waves), reducing two important barriers to model users. In addition, this type of routing is more relevant for simulation of large river systems—more complex approaches usually are reserved for applications to relatively smaller geographic areas because of the increased burden of parameterization and associated uncertainties. In addition to enabling a model user to verify flow at points internal to the basin, as with the subbasin approach, the Muskingum approach enables the flows through the drainage system to be attenuated as needed.

Conclusions

This report described a new extension to the Precipitation-Runoff Modeling System (PRMS) model for simulating the hydrological effects of surface depressions on basin streamflow and presented methods for deriving parameters used to drive these simulations. The surface depression extension is useful in applications where the features are too small or numerous to feasibly be represented as discrete Hydrologic Response Units. An approach for delineating surface depressions, based on Enhanced Thematic Mapper Plus imagery, was demonstrated and compared with two other approaches (which used the National Hydrography Dataset and the National Elevation Dataset, respectively). Estimates of storage volume for the surface depressions were derived by using a regression analysis of National Inventory of Dams data.

The meaning of the impervious area parameter within PRMS and the difference between total impervious area and effective impervious area were discussed. An approach for more accurately estimating values based on the concept of effective imperviousness was demonstrated in conjunction with maps of surface depressions. The report showed that differentiation of surface depressions that are separated from the stream system from those that are attached to it can have a substantial effect on the calculation of this parameter.

This report also described an approach for estimating parameters that quantify the flow of water out of the soil zone of Hydrologic Response Units to the subsurface reservoirs and the groundwater reservoirs. Although these parameters are usually set to PRMS-defined defaults that are constant to all Hydrologic Response Units and adjusted through statistical

calibration, this report demonstrated that values could be set by reclassifying maps of surficial geology into hydrogeological groupings. Even if these values are subsequently adjusted through statistical calibration, using map-based hydrological groupings can improve the realism of the model parameterization by indicating spatial variation across hydrologic response units.

After reviewing the variety of routing options available within PRMS, an extension to PRMS for simulating streamflow routing at a daily time step was developed. The Muskingum streamflow routing extension is useful in applications where the travel time of streamflow exceeds the daily time step of the model. Methods for preparing the parameters used in this extension, implemented in the GIS Weasel, were described.

The application and effect of all of these extensions and methods were demonstrated with an application to the Upper Flint River Basin, a large, unregulated basin in the southeastern United States. The procedure used to evaluate model performance and calibrate model parameters was described. The report discussed and evaluated many aspects of the hydrologic simulation and the preparation of parameter information used to drive it.

References Cited

Alley, W.M., and Veenhuis, J.E., 1983, Effective impervious area in urban runoff modeling: Journal of Hydraulic Engineering-ASCE, v. 109, no. 2, p. 313–319.

Armenakis, C., 2007, A semi-automated approach for the recognition and extraction of water features from Landsat 7 imagery in Northern Canada, in IPY GeoNorth 2007, Proceedings of the First International Circumpolar Conference on Geospatial Sciences and Applications, August 20–24: Yellowknife, Canada, Natural Resources Canada.

Bedient, P.B., and Huber, W.C., 1988, Hydrology and floodplain analysis: Reading, Mass., Addison-Wesley, 763 p.

Chipman, J.W., and Lillesand, T.M., 2007, Satellite-based assessment of the dynamics of new lakes in southern Egypt: International Journal of Remote Sensing, v. 28, no. 19, p. 4365–4379.

Dean, C., 2008, Follow the silt, The New York Times, accessed January 2009, at http://www.nytimes.com/2008/06/24/science/24stream.html?pagewanted=print.

Dempster, G.R., Jr., 1983, Section A. Streamflow/basin characteristics input and update, Instructions for streamflow/basin characteristics file, WATSTORE User's Guide, v. 4: U.S. Geological Survey Open-File Report 79–1336–II, p. 34.

Duan, Q.Y., Gupta, V.K., and Sorooshian, S., 1993, Shuffled complex evolution approach for effective and efficient global minimization: Journal of Optimization Theory and Applications, v. 76, no. 3, p. 501–521.

Duan, Q.Y., Sorooshian, S., and Gupta, V., 1992, Effective and efficient global optimization for conceptual rainfall-runoff models: Water Resources Research, v. 28, no. 4, p. 1015–1031.

Duan, Q.Y., Sorooshian, S., and Gupta, V.K., 1994, Optimal use of the SCE-UA Global Optimization Method for calibrating watershed models: Journal of Hydrology, v. 158, no. 3–4, p. 265–284.

Ford, L.R., and Fulkerson, D.R., 1956, Maximal flow through a network: Canadian Journal of Mathematics, v. VIII, no. 3, p. 399–404.

Freeze, R.A., and Cherry, J.A., 1979, Groundwater: Englewood Cliffs, N.J., Prentice-Hall, 604 p.

Hall, B.M., 1904, Water powers of Alabama, with an appendix on stream measurements in Mississippi: U.S. Geological Survey Water-Supply Paper 107, 253 p.

Hay, L.E., and Clark, M., 2000, Use of atmospheric forecasts in hydrologic models. Part 2: Application to hydrologic models, in D.L. Kane (ed.) Water resources in extreme environments—Proceedings of the American Water Resources Association Spring Specialty Conference, Anchorage, Alaska, May 1–3, 2000: American Water Resources Association, p. 221–226.

Hay, L.E., and Clark, M.P., 2003, Use of statistically and dynamically downscaled atmospheric model output for hydrologic simulations in three mountainous basins in the western United States: Journal of Hydrology, v. 282, no. 1–4, p. 56–75.

Hay, L.E., Clark, M.P., Pagowski, M., Leavesley, G.H., and Gutowski, W.J., 2006a, One-way coupling of an atmospheric and a hydrologic model in Colorado: Journal of Hydrometeorology, v. 7, no. 4, p. 569–589.

Hay, L.E., Clark, M.P., Wilby, R.L., Gutowski, W.J., Leavesley, G.H., Pan, Z., Arritt, R.W., and Takle, E.S., 2002, Use of regional climate model output for hydrologic simulations: Journal of Hydrometeorology, v. 3, no. 5, p. 571–590.

Hay, L.E., Leavesley, G., and Clark, M., 2006b, Use of remotely sensed snow covered area in watershed model calibration for the Sprague River, Oregon, in Joint 8th Federal Interagency Sedimentation Conference and 3rd Federal Interagency Hydrologic Modeling Conference, April 2–6, 2006: Reno, Nevada. http://acwi.gov/hydrology/mtsconfwkshops/conf_proceedings/3rdFIHMC/7D_Hay.pdf.

Hay, L.E., Leavesley, G.H., Clark, M.P., Markstrom, S.L., Viger, R.J., and Umemoto, M., 2006c, Step wise, multiple objective calibration of a hydrologic model for a snowmelt dominated basin: Journal of the American Water Resources Association, v. 42, no. 4, p. 877–890.

Hay, L.E., and McCabe, G.J., 2002, Spatial variability in water-balance model performance in the conterminous United States: Journal of the American Water Resources Association, v. 38, no. 3, p. 847–860.

Hay, L.E., and Umemoto, M., 2006, Multiple-objective stepwise calibration using Luca: U.S. Geological Survey Open-File Report 2006–1323, 28 p.

Homer, C., Dewitz, J., Fry, J., Coan, M., Hossain, N., Larson, C., Herold, N., McKerrow, A., VanDriel, J.N., and Wickham, J., 2007, Completion of the 2001 National Land Cover Database for the conterminous United States: Photogrammetric Engineering and Remote Sensing, v. 73, no. 4, p. 337–341.

Homer, C., Huang, C.Q., Yang, L.M., Wylie, B., and Coan, M., 2004, Development of a 2001 national land-cover database for the United States: Photogrammetric Engineering and Remote Sensing, v. 70, no. 7, p. 829–840.

Hughes, W.B., Freeman, M.C., Gregory, M.B., and Peterson, J.T., 2007, Water availability for ecological needs in the Upper Flint River Basin, Georgia—A USGS Science Thrust Project, *in* Rasmussen, T., Carroll, G.D., and Georgakakos, A., Proceedings of the 2007 Georgia Water Resources Conference, Athens, Georgia, March 27–29, 2007: The University of Georgia, Center for Continuing Education, 3 p.

Jenson, S.K., and Domingue, J.O., 1988, Extracting topographic structure from digital elevation data for geographic information-system analysis: Photogrammetric Engineering and Remote Sensing, v. 54, no. 11, p. 1593–1600.

Leavesley, G.H., Lichty, R.W., Troutman, B.M., and Saindon, L.G., 1983, Precipitation-runoff modeling system—User's manual: U.S. Geological Survey Water-Resources Investigations Report 83–4238, 207 p.

Markstrom, S.L., Niswonger, R.G., Regan, R.S., Prudic, D.E., and Barlow, P.M., 2008, GSFLOW—Coupled groundwater and surface-water flow model based on the integration of the Precipitation-Runoff Modeling System (PRMS) and the Modular Ground-Water Flow Model (MODFLOW-2005): U.S. Geological Survey Techniques and Methods 6–D1, 240 p.

Mastin, M.C., and Vaccaro, J.J., 2002, Documentation of precipitation-runoff modeling system modules for the Modular Modeling System modified for the Watershed and River Systems Management Program: U.S. Geological Survey Open-File Report 02–362, 5 p. (Also available at http://pubs.usgs.gov/of/2002/ofr02362/htdocs/musroute/musroute_prms.htm.)

Morris, S.D., 2005, Flint River, The new Georgia encyclopedia: University of Georgia Press, accessed February 2009, at http://www.georgiaencyclopedia.org/nge/Article.jsp?path=/LandResources/Geography/MajorRiverSystems-1&id=h-3266

Nash, J.E., and Sutcliffe, J.V., 1970, River flow forecasting through conceptual models part I—A discussion of principles: Journal of Hydrology, v. 10, no. 3, p. 282–290.

National Aeronautics and Space Administration, 2009, Landsat 7 science data users handbook, National Aeronautics and Space Administration, accessed January 2009, at http://landsathandbook.gsfc.nasa.gov/handbook.html.

National Oceanic and Atmospheric Administration Cooperative Observer Program, 2009, National Oceanic and Atmospheric Administration, accessed May 2009, at http://www.nws.noaa.gov/om/coop.

Natural Resources Conservation Services, 1996, Fact Sheet: Financial, technical, and educational assistance for landowners: Natural Resources Conservation Services, accessed May 2009, at http://www.nrcs.usda.gov/programs/farmbill/1996/ProgFact.html.

Northeast Georgia Mountain Travel Association, 2005, Grist Mills: Northeast Georgia Mountain Travel Association, accessed January 2009, at http://www.georgiamountains.org/index.php?option=com_content&task=view&id=96&Itemid=61.

Owen, T.M., 1921, History of Alabama and dictionary of Alabama biography: Chicago, S.J. Clarke Publishing Company, 4 v., 1,424 p.

Renwick, W.H., Smith, S.V., Bartley, J.D., and Buddemeier, R.W., 2005, The role of impoundments in the sediment budget of the conterminous United States: Geomorphology, v. 71, no. 1–2, p. 99–111.

Shreve, R.L., 1966, Statistical law of stream numbers: Journal of Geology, v. 74, no. 1, p. 17–37.

Simley, J., 2008, Applying the National Hydrography Dataset: Water Resources Impact, v. 10, no. 1, p. 5–8.

Slack, J.R., and Landwehr, J.M., 1992, Hydro-Climatic Data Network—A U.S. Geological Survey streamflow data set for the United States for the study of climate variations, 1874–1988: USGS Open-File Report 92–129, 193 p.

Slack, J.R., Lumb, A.M., and Landwehr, J.M., 1993, Hydro-Climatic Data Network (HCDN) streamflow data set, 1874–1988: U.S. Geological Survey Water-Resources Investigations Report 93–4076, CD-ROM, accessed March 2007, at http://pubs.usgs.gov/wri/wri934076/.

Smith, S.V., Renwick, W.H., Bartley, J.D., and Buddemeier, R.W., 2002, Distribution and significance of small, artificial water bodies across the United States landscape: Science of the Total Environment, v. 299, no. 1–3, p. 21–36.

Soller, D.R., and Reheis, M.C., 2004, Surficial materials in the conterminous United States: U.S. Geological Survey Open-File Report 03–275, scale 1:5,000,000.

Soller, D.R., Reheis, M.C., Garrity, C.P., and Van Sistine, D.R., 2009, Map database for surficial materials in the conterminous United States: U.S. Geological Survey Data Series 425, scale 1:5,000,000. (Also available at http://pubs.usgs.gov/ds/425/.)

Steuer, J.J., and Hunt, R.J., 2001, Use of a watershed-modeling approach to assess hydrologic effects of urbanization, North Fork Pheasant Branch basin near Middleton, Wisconsin: U.S. Geological Survey Water-Resources Investigations Report 2001–4113, 49 p.

Thomas, D.M., and Benson, M.A., 1970, Generalization of streamflow characteristics from drainage-basin characteristics: U.S. Geological Survey Water-Supply Paper 1975, 55 p.

U.S. Army Corps of Engineers, 2007, National inventory of dams: U.S. Army Corps of Engineers, accessed November 2007, at http://crunch.tec.army.mil/nidpublic/webpages/nid.cfm.

U.S. Geological Survey, 2009, SLC-off products: Background: U.S. Geological Survey, accessed November 2009, at http://landsat.usgs.gov/products_slcoffbackground.php. stations/02349500.html/.

U.S. Geological Survey National Water Information System, 2009, U.S. Geological Survey National Water Information System, accessed May 2009, http://waterdata.usgs.gov/nwis.

Vanderbilt, V.C., Khanna, S., and Ustin, S.L., 2007, Impact of pixel size on mapping surface water in subsolar imagery: Remote Sensing of Environment, v. 109, no. 1, p. 1–9.

Viger, R.J., and Leavesley, G.H., 2007, The GIS Weasel user's manual: U.S. Geological Survey Techniques and Methods, book 6, chap. B4, 201 p.

Vining, K.C., 2002, Simulation of streamflow and wetland storage, Starkweather Coulee Subbasin, North Dakota, water years 1981–98: U.S. Geological Survey Water-Resources Investigations Report 02–4113, 33 p.

Vogelmann, J.E., Howard, S.M., Yang, L.M., Larson, C.R., Wylie, B.K., and Van Driel, N., 2001, Completion of the 1990s National Land Cover Data set for the conterminous United States from Landsat Thematic Mapper data and ancillary data sources: Photogrammetric Engineering and Remote Sensing, v. 67, no. 6, p. 650–662.

Walter, R.C., and Merritts, D.J., 2008, Natural streams and the legacy of water-powered mills: Science, v. 319, no. 5861, p. 299–304.

Wissmar, R.C., Timm, R.K., and Logsdon, M.G., 2004, Effects of changing forest and impervious land covers on discharge characteristics of watersheds: Environmental Management, v. 34, no. 1, p. 91–98.

Yang, L.M., Huang, C.Q., Homer, C.G., Wylie, B.K., and Coan, M.J., 2003, An approach for mapping large-area impervious surfaces—Synergistic use of Landsat-7 ETM+ and high spatial resolution imagery: Canadian Journal of Remote Sensing, v. 29, no. 2, p. 230–240.

Zarriello, P.J., and Barlow, L.K., 2002, Measured and simulated runoff to the lower Charles River, Massachusetts, October 1999–September 2000: U.S. Geological Survey Water-Resources Investigations Report 2002–4129, 89 p.

Publishing support provided by:
Denver Publishing Service Center

For more information concerning this publication, contact:
Chief, Branch of Regional Research, Central Region
Box 25046, Mail Stop 412
Denver, CO 80225
(303) 236-5021

Or visit the USGS National Research Program Web site at:
http://water.usgs.gov/nrp/